Monthly Notices
of the
ROYAL ASTRONOMICAL SOCIETY

MNRAS **469,** 171–192 (2017)
Advance Access publication 2017 April 6

doi:10.1093/mnras/stx798

Transit probabilities in secularly evolving planetary systems

Matthew J. Read,* Mark C. Wyatt and Amaury H. M. J. Triaud
Institute of Astronomy, University of Cambridge, Madingley Road, Cambridge CB3 0HA, UK

Accepted 2017 March 28. Received 2017 March 28; in original form 2017 February 6

ABSTRACT

This paper considers whether the population of known transiting exoplanets provides evidence for additional outer planets on inclined orbits, due to the perturbing effect of such planets on the orbits of inner planets. As such, we develop a semi-analytical method for calculating the probability that two mutually inclined planets are observed to transit. We subsequently derive a simplified analytical form to describe how the mutual inclination between two planets evolves due to secular interactions with a wide orbit inclined planet and use this to determine the mean probability that the two inner planets are observed to transit. From application to Kepler-48 and HD-106315, we constrain the inclinations of the outer planets in these systems (known from radial velocity). We also apply this work to the so-called Kepler Dichotomy, which describes the excess of single transiting systems observed by *Kepler*. We find three different ways of explaining this dichotomy: Some systems could be inherently single, some multiplanet systems could have inherently large mutual inclinations, while some multiplanet systems could cyclically attain large mutual inclinations through interaction with an inclined outer planet. We show how the different mechanisms can be combined to fit the observed populations of *Kepler* systems with one and two transiting planets. We also show how the distribution of mutual inclinations of transiting two-planet systems constrains the fraction of two-planet systems that have perturbing outer planets, since such systems should be preferentially discovered by *Kepler* when the inner planets are coplanar due to an increased transit probability.

Key words: planets and satellites: dynamical evolution and stability.

1 INTRODUCTION

Over the past 20 years, the number of exoplanet detections has soared most notably due to contributions from the *Kepler* space telescope (hereafter *Kepler*). As of 2016 November, *Kepler* has detected 3414 confirmed planets, with 575 existing in multiplanet systems (exoplanet.eu; Schneider et al. 2011). Planet multiplicity provides information on the underlying architecture of planetary systems, such as expected orbital spacing, mutual inclinations and size distributions. Of the multiplanet systems observed by *Kepler*, super-Earth/mini-Neptune-type objects on tightly packed orbits inside of $\sim$200 d are common (Lissauer et al. 2011; Lissauer et al. 2014; Morton et al. 2016). Moreover, such systems are observed to have small inclination dispersions of $\lesssim 5^\circ$ (Lissauer et al. 2011; Fang & Margot 2012; Figueira et al. 2012; Tremaine & Dong 2012; Marmier et al. 2013; Fabrycky et al. 2014).

How representative *Kepler* multiplanet systems are of a common underlying planetary architecture, however, is impeded by *Kepler* preferentially detecting objects that orbit closest to the host star. To generalize *Kepler* systems to an underlying population, it is therefore necessary to account for the inherent probability that transiting systems are observed. Taking into account such probabilities, there appears to be an overabundance of planetary systems with a single transiting planet (Lissauer et al. 2011; Youdin 2011; Johansen et al. 2012; Ballard & Johnson 2016). This is commonly referred to as the 'Kepler Dichotomy'.

It is currently not known what causes this excess. Statistical and *Spitzer* confirmation studies all suggest that the false-positive rate for single transiting objects with $R_\mathrm{p} < 4\ \mathrm{R}_\oplus$ is low at $\lesssim$15 per cent (Morton & Johnson 2011; Fressin et al. 2013; Coughlin et al. 2014; Désert et al. 2015). Perhaps then, there are populations of inherently single planet systems in addition to multiplanet systems that are closely packed and have small inclination dispersions. However, there may also be a population of multiplanet systems where the mutual inclination dispersion is large, such that only a single planet is observed to transit.

The presence of an outer planetary companion may drive this potential large spread in mutual inclinations. Recent *N*-body simulations show that the presence of a wide-orbit planet in multiplanet systems can decrease the number of inner planets that are observed to transit, either through dynamical instability or through inclination excitation (Mustill, Davies & Johansen 2016; Hansen 2017). Beyond a few au, planetary transit probabilities drop to negligible

* E-mail: mjr201@ast.cam.ac.uk

values. It is possible therefore that additional wide-orbit planets could indeed exist in multiplanet systems observed by *Kepler*. Giant planets at a few au have been detected around stars in the general stellar population by a number of radial velocity (RV) surveys (Marmier et al. 2013; Bryan et al. 2016; Rowan et al. 2016; Wittenmyer et al. 2016), with suggested occurrence rates ranging from ∼10 to 50 per cent (Cumming et al. 2008; Mayor et al. 2011; Bryan et al. 2016). Moreover, indirect evidence of undetected giant planets has also been suggested through apsidal alignment of inner RV-detected planets (Dawson & Chiang 2014). As RV studies are largely insensitive to planetary inclinations, it is possible that such wide-orbit planets could be on mutually inclined orbits, which may arise from a warp in the disc (Fragner & Nelson 2010) or due to an excitation by a stellar flyby (Zakamska & Tremaine 2004; Malmberg, Davies & Heggie 2011).

Calculating transit probabilities of multiplanet systems is complex, often requiring computationally exhaustive numerical methods such as Monte Carlo techniques (e.g. Lissauer et al. 2011; Johansen et al. 2012; Becker & Adams 2016; Mustill et al. 2016; Hansen 2017). However, analytical methods can offer a significantly more efficient route for this calculation and allows for coupling with other fundamental analytical theory, such as for the expected dynamical evolution of the system from interplanet interactions. Despite this, however, analytical investigations into the transit probabilities of multiplanet systems for this purpose are relatively sparse (e.g. Ragozzine & Holman 2010; Brakensiek & Ragozzine 2016). Recently, Brakensiek & Ragozzine (2016) showed how differential geometry techniques can be used to calculate multiplanet transit probabilities by mapping transits on to a celestial sphere. In this paper, we perform a similar analysis; however, we focus on regions where pairs of planets can be observed to transit. We also give an explicit analytical form using simple vector relations to describe the boundaries of such transit regions.

The multiplanet systems observed by *Kepler* appear to be mostly stable on long time-scales (Lissauer et al. 2011; Pu & Wu 2015). Dynamical interactions with a potential outer planet on an inclined orbit would therefore be expected to occur on secular time-scales. Recent analytical work by Lai & Pu (2017) suggests that such interactions can lead to large mutual inclinations in an inner planetary system, assuming that the direction of the angular momentum vector of the outer planet is fixed. We build on this work by deriving analytical relations for the mutual inclination that can be induced in an inner planetary system by a general planetary companion. We then simplify this result specifically for when the companion is on a wide orbit. Combining this result with our robust analytical treatment of transit probabilities, we can then derive a simple relation describing how the presence of an outer planetary companion affects the transit probability of an inner system due to long-term interactions.

We also complement recent *N*-body simulations of *Kepler*-like systems interacting with an inclined outer planetary companion shown in Mustill et al. (2016) and Hansen (2017) by using our robust treatment of transit probabilities to consider whether an outer planet with a range of masses, semi-major axes and inclinations can reduce an underlying population of *Kepler* double transiting systems enough to recover the observed number of single transiting systems through long-term interactions only. We also investigate whether the presence of specific wide-orbit planets in multiplanet systems preferentially predicts single transiting planets with a given distribution of radii and semi-major axes.

In Section 2, we overview our semi-analytical method for calculating the transit probability of two mutually inclined planets. In Section 3, we derive a simplified form to describe the evolution of the mutual inclination between two planets due to the presence of an outer planetary companion. We show how this mutual inclination affects the transit probability of the two inner planets in Section 4. In Section 5, we apply this work to Kepler-56, Kepler-68, HD 106315 and Kepler-48 to place constraints on the inclination of the outer planets in these systems. In Section 6, we investigate whether a wide-orbit planet in *Kepler* systems can decrease the number of observed two-planet transiting systems enough to recover the observed abundances of single transiting systems. We finally discuss this work in Section 7 and conclude in Section 8.

2 SEMI-ANALYTICAL TRANSIT PROBABILITY

A planet on a circular orbit with a semi-major axis a and radius R_p subtends a band of shadow across the celestial sphere due its orbital motion. We refer to this band of shadow as the *transit region* (Ragozzine & Holman 2010; Brakensiek & Ragozzine 2016). The probability that an observer will view an individual transit event of this planet, assuming that the system is viewed for long enough, is equal to the number of viewing vectors that intersect the transit region, divided by the total number of possible viewing vectors. Perhaps more intuitively, this is equivalent to the surface area of the transit region divided by the total surface area of the celestial sphere.

To calculate the area of a transit region on the celestial sphere, first, consider that the area of a given surface element (S) on a unit sphere is equal to

$$S = \int_0^{\theta_0}\int_0^{\phi_0} \sin\theta' \mathrm{d}\theta' \mathrm{d}\phi' = \left[1-\cos\theta'\right]_0^{\theta_0}\left[\phi'\right]_0^{\phi_0}, \quad (1)$$

where θ' is the polar angle and ϕ' is the azimuthal angle. A given area on the celestial sphere can therefore be represented on a 2D plane of $1-\cos\theta'$ versus ϕ', from $0 \rightarrow 2$ and $0 \rightarrow 2\pi$, respectively, such that the 2D plane has a total surface area of 4π. Below we show how the boundaries of a given transit region traverses this 2D plane. This allows for the area contained within these boundaries and therefore the associated transit probability to be calculated.

2.1 Single-planet case

Consider some fixed reference plane where $[\hat{\boldsymbol{X}}, \hat{\boldsymbol{Y}}]$ define a pair of orthogonal directions in this plane, and $\hat{\boldsymbol{Z}}$ defines a direction orthogonal to this plane, as shown in Fig. 1. The fixed reference frame in Fig. 1 is assumed to be centred on a host star with radius R_*. The line of sight of an observer is considered to be randomly oriented over the surface of a celestial sphere with respect to this fixed reference plane. Now consider that the orbital plane of a planet with a semi-major axis a and radius R_p is inclined to the fixed reference plane by Δi, with the intersection between the two planes occurring along the $\hat{\boldsymbol{X}}$ direction. The direction of the normal of the orbital plane is given by $\hat{\boldsymbol{n}}$. The position of a planet in the orbital plane is defined by the direction $\hat{\boldsymbol{r}}$, which makes the angles θ and ϕ with the $\hat{\boldsymbol{Z}}$ and $\hat{\boldsymbol{X}}$ directions, respectively. Hence, $\hat{\boldsymbol{r}}$ traces the centre of the transit region with respect to the fixed reference plane. As $\hat{\boldsymbol{n}} \cdot \hat{\boldsymbol{r}} = 0$, where $\hat{\boldsymbol{n}} = [0, \sin\Delta i, \cos\Delta i]$ and $\hat{\boldsymbol{r}} = [\sin\theta\cos\phi, \sin\theta\sin\phi, \cos\theta]$, it follows that

$$-\sin\Delta i \sin\theta \sin\phi + \cos\Delta i \cos\theta = 0. \quad (2)$$

Hence, equation (2) defines how the centre of a transit region inclined to a fixed reference plane by Δi traverses a celestial sphere.

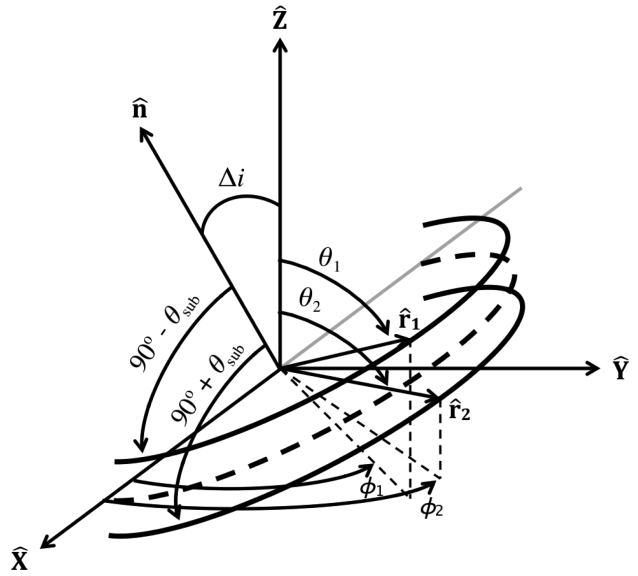

Figure 1. The coordinate system used to show how a transit region traverses the surface of a celestial sphere. The dashed line represents an orbital plane inclined to a fixed reference plane by Δi. The direction $\hat{\boldsymbol{n}}$ is normal to the orbital plane. The directions $\hat{\boldsymbol{r}}$, $\hat{\boldsymbol{r}}_1$ and $\hat{\boldsymbol{r}}_2$ trace the central, lower and upper boundaries of a transit region, respectively.

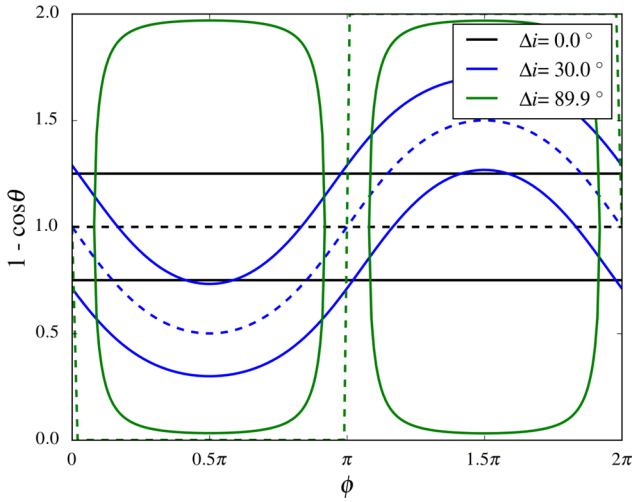

Figure 2. The surface of a celestial sphere represented on a 2D plane. The dotted lines represent the centre of a transit region for a planet inclined to a fixed reference plane by Δi. The solid lines refer to the boundaries of such transit regions for when $R_*/a = 0.25$. The areas within these transit regions are identical, giving an identical single transit probability equal to 0.25.

This is shown by the dashed lines in Fig. 2 for different values of Δi, where the surface area of the celestial sphere is shown on a 2D plane defined by equation (1). We note that at the special case where $\Delta i = 90^\circ$, ϕ can take only values of 0 or π.

Similarly, the directions that define the boundaries of the transit region can be given by $\hat{\boldsymbol{r}}_1$ and $\hat{\boldsymbol{r}}_2$, which makes the angles θ_1, θ_2 and ϕ_1, ϕ_2 with the $\hat{\boldsymbol{Z}}$ and $\hat{\boldsymbol{X}}$ directions, respectively, shown in Fig. 1. The boundaries of the transit region also subtend an angle $\pm\theta_{\rm sub}$ from the orbital plane, where $\sin\theta_{\rm sub} = R_*/a$ assuming $R_* \gg R_{\rm p}$ (Borucki & Summers 1984). As $\hat{\boldsymbol{r}}_1 = [\sin\theta_1\cos\phi_1, \sin\theta_1\sin\phi_1, \cos\theta_1]$, $\hat{\boldsymbol{r}}_2 = [\sin\theta_2\cos\phi_2, \sin\theta_2\sin\phi_2, \cos\theta_2]$ and $\hat{\boldsymbol{n}}\cdot\hat{\boldsymbol{r}}_1 = R_\star/a$ and $\hat{\boldsymbol{n}}\cdot\hat{\boldsymbol{r}}_2 = -R_\star/a$, it follows that

$$-\sin\Delta i\sin\theta_1\sin\phi_1 + \cos\Delta i\cos\theta_1 = R_\star/a, \quad (3)$$

$$-\sin\Delta i\sin\theta_2\sin\phi_2 + \cos\Delta i\cos\theta_2 = -R_\star/a. \quad (4)$$

Hence, equations (3) and (4) describe how the lower and upper boundaries of the transit region for a planet inclined to a fixed reference plane by Δi traverse a celestial sphere. The solid lines in Fig. 2 show these boundaries for different values of Δi, where $R_*/a = 0.25$. This value of R_*/a might be considered to be unrealistically large and is used for demonstration purposes only. In Appendix A, we further discuss how the values of (θ_1, ϕ_1) and (θ_2, ϕ_2) in equations (3) and (4), respectively, would be expected to change as Δi is increased from $\Delta i = 0 \rightarrow 90^\circ$.

An integration between the upper and lower boundaries of a transit region divided by the total surface area of the celestial sphere gives the associated *single transit probability* of the planet (R_*/a, Borucki & Summers 1984). All of the transit regions shown in Fig. 2 for different Δi therefore contain identical areas and hence have identical single transit probabilities equal to 0.25. We note that if the planet has a non-negligible radius, then the single transit probability becomes $(R \pm R_{\rm p})/a$ for grazing and full transits, respectively. Throughout this work, however, we assume that $R_{\rm p} \ll R_*$.

2.2 Two-planet case

Consider now a system containing two planets, both of which are on circular orbits with semi-major axes and radii of a_1, a_2 and $R_{\rm p1}$, $R_{\rm p2}$, respectively, where $a_1 < a_2$ and the orbital planes are mutually inclined by Δi (we give an exact definition for mutual inclination in Section 3). The probability that a randomly oriented observer will view both planets to transit (assuming the system is observed for long enough) is equal to the overlap area between the transit regions of both planets, divided by the total area of the celestial sphere. We refer to this probability as the *double transit probability*.

Therefore, using equations (3) and (4) to find where the boundaries of the transit regions of each planet intersect, an outline of the overlap between the transit regions can be determined. The area of this overlap can subsequently be calculated by an appropriate integration, which when divided by 4π gives the double transit probability. How the double transit probability changes as a function of Δi is shown by the blue line in Fig. 3, for when $R_*/a_1 = 0.2$ and $R_*/a_2 = 0.1$. We note that this result is consistent, regardless of the choice of reference plane and the orientation of the orbital planes of both planets with respect to this reference plane (see Ragozzine & Holman 2010 for a further discussion). That is, the double transit probability depends on the mutual inclination between the two planets only (in addition to the physical size of the respective transit regions).

Depending on the value of Δi, the double transit probability (hereafter P) can be split into three regimes (also discussed in Ragozzine & Holman 2010; Brakensiek & Ragozzine 2016):

(1) For low values of Δi, the transit region of the outer planet is enclosed within that of the inner planet. The double transit probability is therefore equal to R_*/a_2.

(2) Δi is large enough that the transit region of one planet is no longer fully enclosed inside the other; however, there is still partial overlap for all azimuthal angles on the celestial sphere. The transition to this regime occurs for a value of $\Delta i = I_1$, which causes θ_1

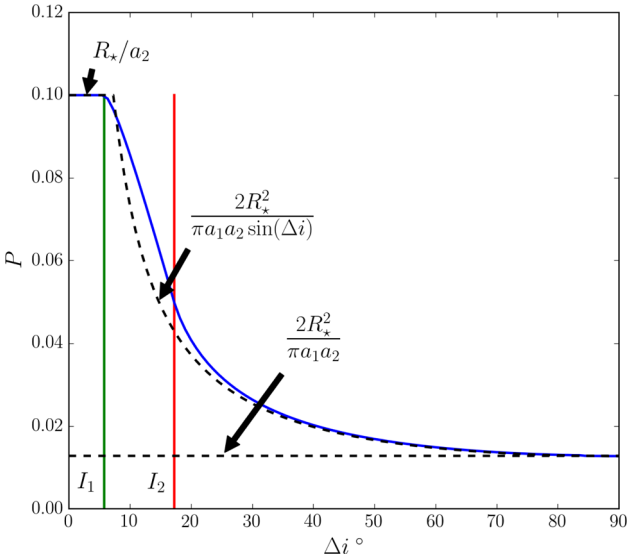

Figure 3. The double transit probability as a function of mutual inclination between two planets from our method (blue line) for when $R_*/a_1 = 0.2$ and $R_*/a_2 = 0.1$. The dashed black lines represent the associated analytical estimate given by equation (7). The green and red lines represent which inclination causes the double transit probability to go from regime 1 to 2 and regime 2 to 3, with the regimes being defined in Section 2.2.

in equation (3) for both planets to be equal at $\phi_1 = \pi/2$. Evaluating equation (3) at this point gives

$$\sin I_1 = -\kappa_2(1-\kappa_1^2)^{1/2} + \kappa_1(1-\kappa_2^2)^{1/2}, \tag{5}$$

where $\kappa_1 = R_*/a_1$ and $\kappa_2 = R_*/a_2$, for simplicity. We note that determining the overlap area of the two transit regions with an exact analytical expression in this regime is difficult and is commonly calculated by Monte Carlo techniques (e.g. Ragozzine & Holman 2010; Johansen et al. 2012; Becker & Adams 2016; Mustill et al. 2016; Hansen 2017).

(3) For large Δi, the transit regions overlap only at the intersection of the two orbital planes. The transition to this regime occurs when $\Delta i = I_2$, where θ_1 for the inner planet is equal to θ_2 for the outer planet at $\phi_1 = \phi_2 = \pi/2$. Evaluating equation (3) and (4) here gives

$$\sin I_2 = \kappa_2(1-\kappa_1^2)^{1/2} + \kappa_1(1-\kappa_2^2)^{1/2}. \tag{6}$$

The values of I_1 and I_2 are shown by the green and red lines, respectively, in Fig. 3. If it is assumed that the transit region overlap in regime 3 can be represented as a 2D parallelogram, Ragozzine & Holman (2010) showed that the double transit probability can be approximated by[1]

$$P = \frac{2R_\star^2}{\pi a_1 a_2 \sin \Delta i}. \tag{7}$$

For large Δi therefore, the double transit probability predicted by equation (7) tends to a value of $2R_\star^2/\pi a_1 a_2$. We show equation (7) as the black dashed line in Fig. 3. We note that in Ragozzine & Holman (2010) it was assumed that the double transit probability transitions straight from regime (1) to (3) at $\Delta i = \arcsin\left(\frac{2}{\pi}\min(R_\star/a_1, R_\star/a_2)\right)$.[1]

For $\Delta i > I_2$ our method predicts a double transit probability that agrees well with the analytical estimate from Ragozzine & Holman (2010). However, there is a clear discrepancy for $I_1 < \Delta i < I_2$, for when there is partial overlap between the transit regions at all azimuthal angles. This highlights the need for semi-analytical methods like the one suggested here over purely analytical relations, to robustly calculate double transit probabilities at all values of Δi. We note that our method also agrees well with the Monte Carlo treatment of double transit probabilities shown in Ragozzine & Holman (2010).

Calculating transit probabilities using the method outlined here is significantly more computationally efficient than equivalent Monte Carlo methods, as it is necessary only to solve combinations of equations (3) and (4) for different planets to find where transit regions overlap. From integrating around this overlap, the associated double transit probability is also exact and not subject to Monte Carlo noise effects from undersampling the total number of line-of-sight vectors.

3 SECULAR INTERACTIONS

3.1 *N*-planet system

Consider a system of N secularly interacting planets in which planet j has a semi-major axis a_j and mass m_j. The inclination and longitude of ascending node of planet j are given by I_j and Ω_j, respectively, and can be combined into the associated complex inclination $y_j = I_j e^{i\Omega_j}$. Assuming that the vector involving all the planet's orbital planes is given by $\boldsymbol{y} = [y_1, y_2, \ldots, y_N]$, the evolution of complex inclinations in the low inclination and eccentricity limit can be given by Laplace–Lagrange theory in the form

$$\dot{\boldsymbol{y}} = i\mathbf{B}\boldsymbol{y} \tag{8}$$

(Murray & Dermott 1999), where $\mathbf{B}$ is a matrix with elements given by

$$B_{jk} = \frac{1}{4} n_j \left(\frac{m_k}{M_\star + m_j}\right) \alpha_{jk}\tilde{\alpha}_{jk} b_{3/2}^{(1)}(\alpha_{jk}) \quad (j \neq k),$$

$$B_{jj} = -\sum_{k=1, j\neq k}^{N} B_{jk}, \tag{9}$$

where j and k are integers associated with each planet, M_* and m_i are the masses of the star and planet i, n_j is the mean motion of planet j, where $n_j^2 a_j^3 = G(M_\star + m_j)$, $\alpha_{jk} = \tilde{\alpha}_{jk} = a_j/a_i$ for $a_j < a_k$ and $\alpha_{jk} = a_k/a_j$ and $\tilde{\alpha}_{jk} = 1$ otherwise, and $b_{3/2}^{(1)}(\alpha_{jk})$ corresponds to a Laplace coefficient given by

$$b_s^{(\nu)}(\alpha) = \frac{1}{\pi}\int_0^{2\pi} \frac{\cos(\nu x)\mathrm{d}x}{(1 - 2\alpha\cos(x) + \alpha^2)^s} \qquad \alpha < 1. \tag{10}$$

Equation (8) can be solved to show that the evolution of $\boldsymbol{y}$ is given by a superposition of eigenmodes associated with each eigenfrequency f_i of the matrix $\mathbf{B}$:

$$y_j(t) = \sum_{k=1}^{N} I_{jk} e^{i(f_k t + \gamma_k)}, \tag{11}$$

where I_{jk} are the eigenvectors of $\mathbf{B}$ scaled to initial boundary conditions and γ_k is an initial phase term. If it is assumed that all objects are spherically symmetric, additional terms in the diagonal elements of $\mathbf{B}$ in equation (9) (e.g. stellar oblateness) need not be included. A choice of reference frame for the inclination also becomes arbitrary, leading to one of the eigenfrequencies equalling zero (c.f. Murray & Dermott 1999). It is meaningful therefore to describe only a *mutual inclination* between pairs of planets, with

[1] For greater accuracy, we include a $2/\pi$ factor here, which is not included in Ragozzine & Holman (2010).

the invariable plane commonly being chosen as a reference plane. The invariable plane is defined as being perpendicular to the total angular momentum vector of a system. The mutual inclination is then the angle between individual angular momentum vectors of a pair of planets. The inclination solution described by equation (11) also becomes simplified when the invariable plane is taken as a reference plane as the eigenvector associated with the zero value eigenfrequency is also equal to zero.

3.2 Two-planet system with an inclined companion

Consider the same general two-planet system from Section 2.2. Assume that the two planets are initially coplanar. Consider now a third planet on an external circular orbit, with a mass and semi-major axis of m_3 and a_3, respectively, such that $a_3 > a_2$. The orbital plane of this external planet is initially mutually inclined to the inner planets by Δi. We assume that each of the planets interacts through secular interactions only, and that inclinations and eccentricities remain small, allowing for the application of Laplace–Lagrange theory. Assuming that the invariable plane is taken as a fixed reference plane, the initial inclination of the third planet i_3 is given by

$$i_3 = \arctan\left[\frac{(L_1 + L_2)\sin\Delta i}{L_3 + (L_1 + L_2)\cos\Delta i}\right],$$

where $L_j = m_j a_j^{1/2}$ and is proportional to the angular momentum in the low eccentricity limit. The initial inclination of the inner planets with respect to the invariable plane is therefore $i_1 = \Delta i - i_3$.

From equation (11) the complex inclination of each of the inner two planets with respect to the invariable plane evolves in the form of

$$\begin{aligned} y_1 &= I_{11}\mathrm{e}^{\mathrm{i}(f_1 t+\gamma_1)} + I_{12}\mathrm{e}^{\mathrm{i}(f_2 t+\gamma_2)},\\ y_2 &= I_{21}\mathrm{e}^{\mathrm{i}(f_1 t+\gamma_1)} + I_{22}\mathrm{e}^{\mathrm{i}(f_2 t+\gamma_2)}, \end{aligned} \tag{12}$$

where y_1 and y_2 are the complex inclinations of the innermost and second innermost planets, respectively. The evolution of the mutual inclination between the inner pair of planets is hence given by

$$y_1 - y_2 = (I_{11} - I_{21})\mathrm{e}^{\mathrm{i}(f_1 t+\gamma_1)} + (I_{12} - I_{22})\mathrm{e}^{\mathrm{i}(f_2 t+\gamma_2)}. \tag{13}$$

The $t = 0$ boundary conditions give $\gamma_1 = \pi$ and $\gamma_2 = 0$. Also as $y_1(t = 0) = y_2(t = 0) = i_1$, it follows from equation (12) that $I_{11} - I_{21} = I_{12} - I_{22}$. The evolution of the mutual inclination from equation (13) is therefore is equivalent to

$$y_1 - y_2 = (I_{12} - I_{22})\left(\mathrm{e}^{\mathrm{i}(f_1 t+\pi)} + \mathrm{e}^{\mathrm{i}f_2 t}\right). \tag{14}$$

Hence, the evolution of the instantaneous mutual inclination between the inner pair of planets, $\Delta i_{12} = |y_1 - y_2|$, can be calculated if the first and second elements of the eigenvector associated with the f_2 eigenfrequency are known. In Appendix B, we fully solve equation (8) to give I_{12} and I_{22} in terms of physical variables. Here we simply say that

$$y_1 - y_2 = \Delta i K\left[\mathrm{e}^{\mathrm{i}(f_1 t+\pi)} + \mathrm{e}^{\mathrm{i}f_2 t}\right], \tag{15}$$

where K is dependent on the masses and semi-major axes of the three planets, shown explicitly in Appendix B. We note that the maximum value of $K \approx 1$, implying that the maximum value of the mutual inclination between the inner pair of planets from equation (14) is twice the initial mutual inclination with the external third planet, i.e. $\max|\Delta i_{12}| = 2\Delta i$. For given values of masses and semi-major axes of the inner pair of planets therefore, the evolution of the mutual inclination between them is dependant on three quantities, a_3, m_3 and Δi.

The left-hand panels of Fig. 4 show how $\max|\Delta i_{12}|$ changes as a function of different combinations of a_3, m_3 and Δi in equation (15) for an example system where a_1, $a_2 = 0.2$, 0.5 au and m_1, $m_2 = 10\ \mathrm{M}_\oplus$. We note that the assumptions of Laplace–Lagrange theory are expected to break down when $\Delta i \gg 20^\circ$. Larger inclinations are included for demonstration purposes only. It is evident that as the third planet tends to a limit where it is on a wide orbit, with a low mass and low initial mutual inclination, the maximum mutual inclination between the inner pair of planets becomes small as one might expect.

3.3 Companion wide orbit approximation

In Section 4, we look to investigate how the evolving mutual inclination between the inner pair of planets affects the associated double transit probability, for the specific case where the external third planet is assumed to be on a wide orbit. For $a_3 \gg a_1$, a_2, certain individual and combinations of **B** matrix elements from equation (9) become small, and we find that equation (15) can be simplified to

$$y_1 - y_2 \approx \Delta i K_{\mathrm{simp}}\left[\mathrm{e}^{\mathrm{i}(f_1 t+\pi)} + \mathrm{e}^{\mathrm{i}f_2 t}\right], \tag{16}$$

where

$$K_{\mathrm{simp}} = \frac{3m_3 a_2^{7/2}}{m_2 a_1^{1/2} a_3^3}\frac{1}{b^1_{3/2}\left(\frac{a_1}{a_2}\right)(1 + (L_1/L_2))}. \tag{17}$$

Here it is assumed that as $a_3 \gg a_1$, a_2, certain Laplace coefficients from the **B** matrix elements can be simplified, specifically $b^1_{3/2}(\alpha) \approx 3(\alpha)$ (Murray & Dermott 1999). Similar simplifications can be made to each of the eigenfrequencies, for which

$$\begin{aligned} f_1 &\approx -\frac{\pi m_2 a_1^{1/2}}{2M_\star^{1/2} a_2^2} b^1_{3/2}\left(\frac{a_1}{a_2}\right)(1 + L_1/L_2),\\ f_2 &\approx -\frac{3\pi m_3 a_2^{3/2}}{2M_\star^{1/2} a_3^3}\frac{1}{1 + L_1/L_2}. \end{aligned} \tag{18}$$

As equation (15) shows that the maximum value of the mutual inclination between the inner pair of planets cannot be larger than twice the initial mutual inclination with the wide-orbit planet ($\max|\Delta i_{12}| \not> 2\Delta i$), we assume that the maximum value of the mutual inclination between the inner two planets predicted by equation (16) is

$$\begin{aligned} \max|\Delta i_{12}| &\approx 2\Delta i K_{\mathrm{simp}} \quad \text{for } K_{\mathrm{simp}} < 1,\\ &\approx 2\Delta i \quad \text{otherwise.} \end{aligned} \tag{19}$$

The right-hand panels of Fig. 4 show $\max|\Delta i_{12}|$ predicted by equations (19) and (17) using the same planet parameters as shown in the left-hand panels. We find that when $a_3 \gtrsim 1.25$ au, the simplified form for $\max|\Delta i_{12}|$ from equations (19) and (17) agrees with the full Laplace–Lagrange solution to within ∼25 per cent for all values of m_3 and Δi. For $a_3 \sim 1$ au, the simplified form of $\max|\Delta i_{12}|$ begins to break down, and equation (19) can underestimate $\max|\Delta i_{12}|$ from the full Laplace–Lagrange solution by up to a factor of 2.

This estimate is similar to the result derived by Lai & Pu (2017), who assumed that the angular momentum vector direction of the outer inclined planet is fixed in time. They find that the maximum mutual inclination that can be induced in an inner pair of planets depends on the strength of the coupling between them (parametrized by ϵ_{12} in their equation 12). Assuming that inclinations are small, we find that equation (19) agrees with the equivalent prediction of

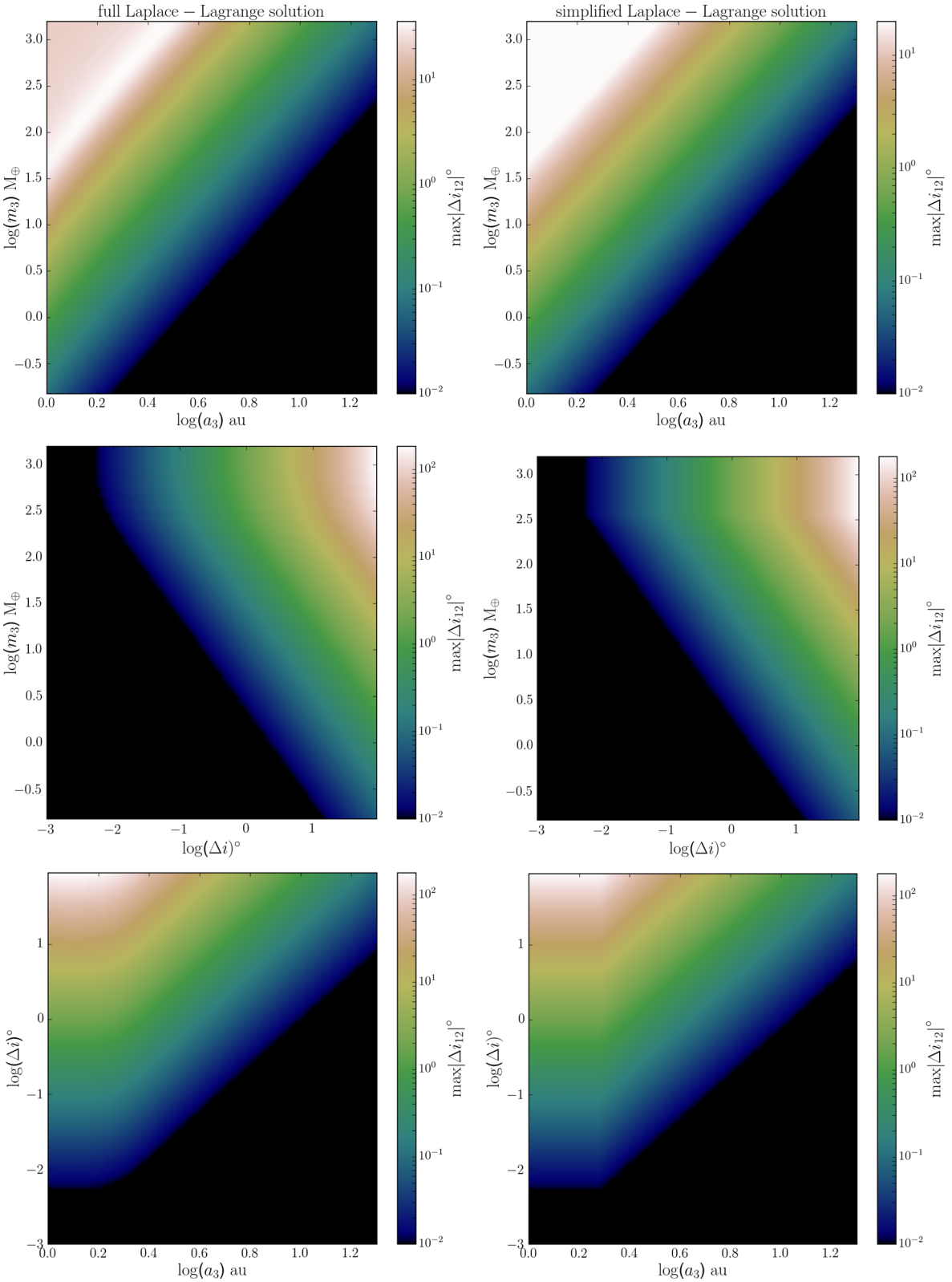

Figure 4. The maximum mutual inclination, $\max|\Delta i_{12}|$, between two planets on circular, initially coplanar orbits with a semi-major axis of 0.2 and 0.5 au and masses of 10 $M_\oplus$, from the secular interaction with an outer third planet. The value of $\max|\Delta i_{12}|$ calculated by the full Laplace–Lagrange solution from equation (15) is given by the colour scale in the left-hand panels. The right-hand panel colour scales give $\max|\Delta i_{12}|$ calculated by the simplified Laplace–Lagrange solution for when $a_3 \gg a_1$, a_2, given by equations (16) and (17). For the top panels, $\Delta i = 10^\circ$, for the middle panels, $m_3 = M_\mathrm{J}$, and for the bottom panels, $a_3 = 2$ au. It is important to note that the assumptions of Laplace–Lagrange theory break down when $\Delta i \gg 20^\circ$. Larger inclinations are included in this figure only to aid comparison between $\max|\Delta i_{12}|$ predicted by the full and simplified Laplace–Lagrange theory solutions.

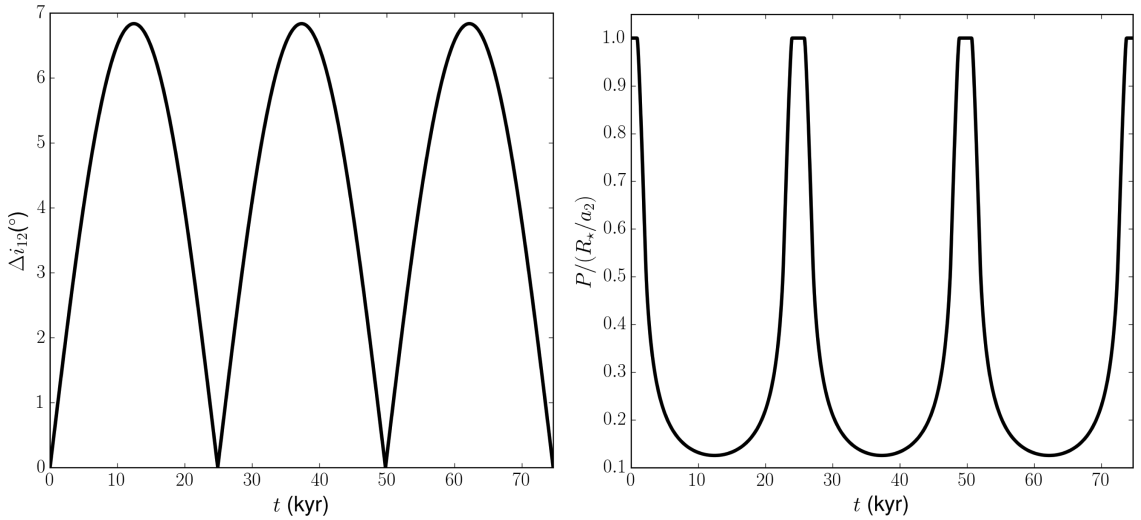

Figure 5. Left-hand panel: the evolution of the mutual inclination of the two inner planets considered in Fig. 4 due to secular interactions with a third planet with $a_3 = 2$ au, $m_3 = 1 M_J$ and $\Delta i = 5^\circ$. Right-hand panel: the associated evolution of the double transit probability.

$\max|\Delta i_{12}|$ from Lai & Pu (2017) if $K_{\rm simp} = \epsilon_{12}$. Indeed, $K_{\rm simp}$ and ϵ_{12} are almost identical despite the different derivation techniques (e.g. we derive the full Laplace–Lagrange solution and then simplified assuming $a_3 \gg a_1, a_2$), apart from $K_{\rm simp}$ contains an additional factor of $a_1^{1/2} a_2^{3/2}$, whereas ϵ_{12} contains a factor of $(a_2^2 - a_1^2)$. By considering different combinations of a_1 and a_2 and comparing to the value of $\max|\Delta i_{12}|$ given by the full solution in Appendix B, we find that neither equations (19) and (17) nor the equivalent equation from Lai & Pu (2017) is favoured as a more accurate approximation, since which is closer to the full solution depends on the exact parameters.

4 COMBINING TRANSIT PROBABILITIES WITH SECULAR THEORY

Considering two inner, initially coplanar planets and an outer inclined planetary companion, we combine the analysis of transit probabilities from Section 2 with secular interactions from Section 3 in two main ways. First, in Section 4.1, we assume that the outer planet is not necessarily on a wide orbit. The evolution of the mutual inclination between the inner planets is therefore assumed to be given by the full Laplace–Lagrange solution derived in equation (15). The double transit probability of the inner two planets during this evolution is then calculated through the method outlined in Section 2. This provides the most accurate prediction for how the double transit probability of two inner planets evolves (in the low inclination limit) considering a given outer planetary companion. We make use of this method for a detailed discussion of how an outer planet affects an inner population of *Kepler* systems in Section 6.

Secondly, in Section 4.2, we assume that the outer planetary companion is on a significantly wide orbit. The evolution of the mutual inclination between the inner two planets is therefore given by equations (16) and (17). Here we look to give a simple analytical form to describe the double transit probability of two inner planets, due to secular interactions with a given outer planetary companion. We make use therefore of simple analytical relations such as equation (7) to describe double transit probabilities. Comparing with the work in Section 4.1 allows for the accuracy of these approximations to be judged. We demonstrate in Section 5 how simple constraints can be placed on the inclination of an outer companion in specific systems using this method.

4.1 Two-planet system with an inclined companion

From Fig. 3 it is clear that if the amplitude of the mutual inclination between the inner two planets is large, then the associated double transit probability, P, will only be at a maximum value for a small proportion of the secular evolution. The presence of an outer inclined planet may therefore result in a significant reduction in the mean double transit probability $\langle P \rangle$ on long time-scales. Fig. 5 shows how both the mutual inclination and the double transit probability evolve with time for two inner planets from Fig. 4, which are perturbed by an outer planetary companion with a semi-major axis, mass and inclination of $a_3 = 2$ au and $m_3 = 1 M_J$ and $\Delta i = 5^\circ$, respectively. Indeed, P is only at a maximum value for a small proportion of the secular evolution, leading to a significant reduction in $\langle P \rangle$ compared with if the outer planet were not present.

Furthermore, the left-hand panels of Fig. 6 show how $\langle P \rangle$ changes due to perturbations from an outer planet with the same range of parameters as considered in Fig. 4. As one may expect, through comparing the left-hand panels of Figs 4 and 6, an outer planet that induces a large value of $\max|\Delta i_{12}|$ also causes a significant reduction in the mean double transit probability of the inner two planets and vice versa for small values of $\max|\Delta i_{12}|$.

The left-hand panels of Fig. 6 also suggest a clear boundary of a_3, m_3 and Δi, above which the outer planet causes $\langle P \rangle$ to be significantly reduced and below which $\langle P \rangle$ is unchanged. From Fig. 3, the double transit probability of the two inner planets can be considered to be significantly reduced when $\Delta i_{12} > I_1$, where I_1 is given by equation (5). We assume therefore that the boundary where $\langle P \rangle$ is significantly reduced occurs when $\max|\Delta i_{12}| \approx I_1$. The values of a_3, m_3 and Δi that give this boundary are shown by the black lines in the left-hand panels of Fig. 6.

4.2 Companion wide orbit approximation

Considering the simplified evolution of the mutual inclination from equations (16) and (17) for when $a_3 \gg a_1, a_2$, here we estimate the value of the mean double transit probability itself. We assume

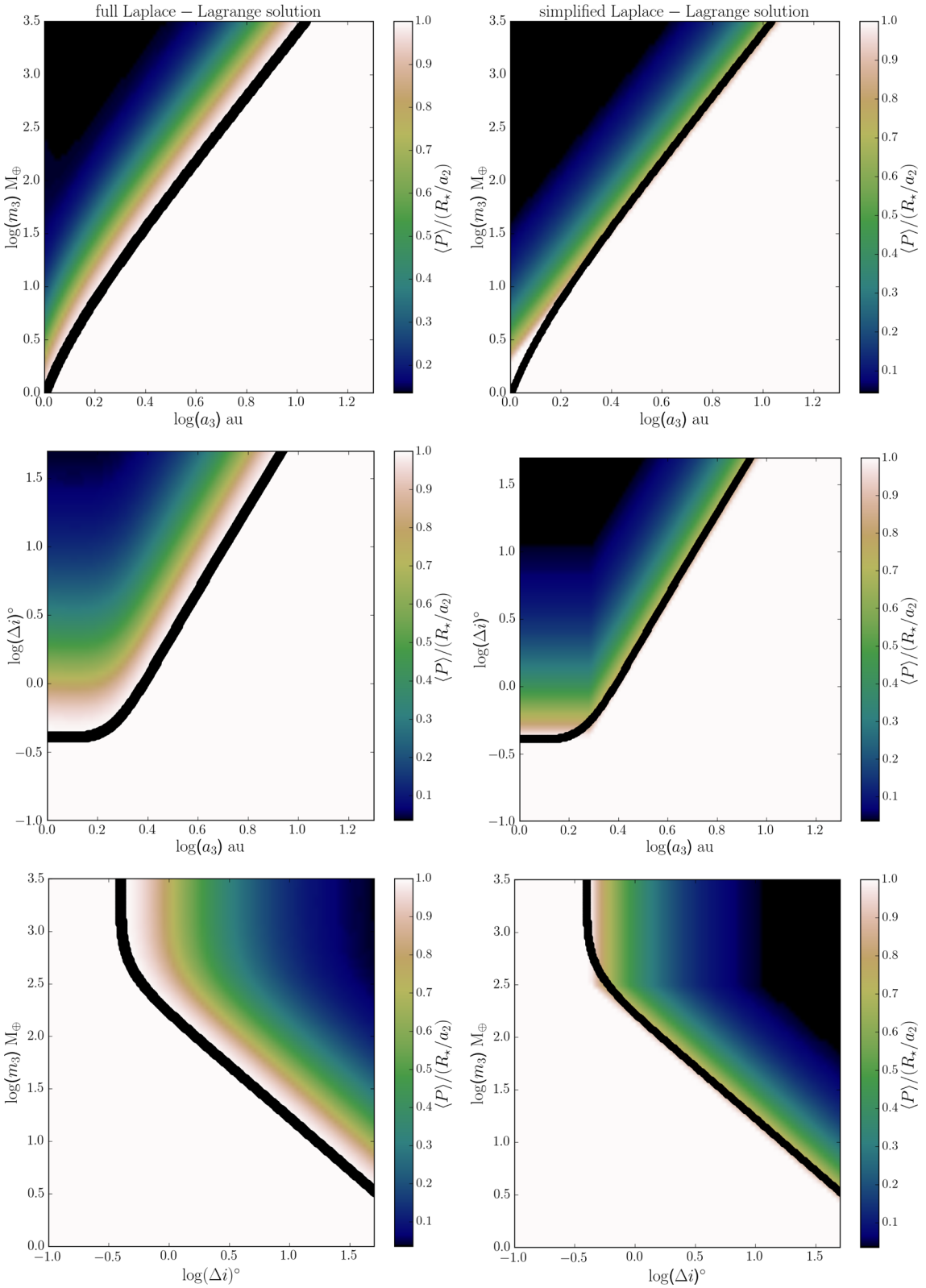

Figure 6. The mean double transit probability of two planets $\langle P \rangle$ from Fig. 4, which are being secularly perturbed by a third planet on a mutually inclined orbit according to the full Laplace–Lagrange solution (left-hand panels) and the simplified Laplace–Lagrange solution for when the third planet is assumed to be on a wide orbit. The black lines show the boundary where the maximum mutual inclination between the inner planets exceeds I_1 from equation (5) and $\langle P \rangle$ is assumed to be significantly reduced. The black lines on the respective left- and right-hand panels are identical and included to aid comparison. As noted in Fig. 4, Laplace–Lagrange theory is expected to break down for $\Delta i \gg 20^\circ$. Larger inclinations are included here only for demonstration purposes only.

that $\langle P \rangle$ is dominated by the maximum or minimum value of the double transit probability, $P_{\rm max}$ and $P_{\rm min}$, respectively, depending on whether $\max|\Delta i_{12}|$ is greater than I_1. We assume that $I_1 \approx R_*/a_1 - R_*/a_2$ from equation (5) for R_*/a_1, $R_*/a_2 \ll 1$. From Fig. 3, the value of $P_{\rm max} = R_*/a_2$; however, a value of $P_{\rm min}$ is more difficult as no specific analytical estimate exists. We therefore assume that $P_{\rm min}$ can be given by the estimate from Ragozzine & Holman (2010) shown by equation (7). We note that this approximation for $P_{\rm min}$ would be expected to break down if $\max|\Delta i_{12}|$ predicts partial overlap between the transit regions of the inner planets for all azimuthal angles (see Fig. 3). Assuming that the masses and semi-major axes of all the planets are known, in addition to the inclination of the outer planet and that $\max|\Delta i_{12}|$ is given by the simplified Laplace–Lagrange solution from equation (19), $\langle P \rangle$ can be estimated by

$$\begin{aligned} \langle P \rangle &\approx R_\star/a_2 \quad \text{for } \max|\Delta i_{12}| < R_\star/a_1 - R_\star/a_2 \\ &\approx \frac{2R_\star^2}{\pi a_1 a_2 \sin(\max|\Delta i_{12}|)} \quad \text{otherwise.} \end{aligned} \tag{20}$$

The right-hand panels of Fig. 6 show the value of $\langle P \rangle$ predicted by equation (20), using the same planet parameters as those in the left-hand panels. The black lines are identical to those in the left-hand panels of Fig. 6 and are included to aid comparison between both sides of the figure.

The above assumptions bias the double transit probability towards spending a greater proportion of the secular evolution at $P_{\rm min}$. As such, equation (20) can under predict $\langle P \rangle$, by a factor of up to 4 when comparing the left- and right-hand panels of Fig. 6. We suggest therefore that equation (20) should be used as a first-order approximation of $\langle P \rangle$ only.

5 APPLICATION TO SPECIFIC SYSTEMS

Here we consider real systems observed to have both transiting planets and an additional outer, non-transiting planet. Due to the inherent faintness of *Kepler* stars, follow-up observations to detect non-transiting planets, namely by RV studies, are challenging. Thus, the number of systems observed with such architectures are relatively sparse. We consider three of these systems: Kepler-56, Kepler-68 and Kepler-48, in addition to HD 106315. As RV surveys are largely insensitive to planetary inclinations, we apply equation (20) with equation (17) to place constraints on the inclination of the non-transiting planets in these systems.

Assume that, as the transiting planets are indeed transiting, the mean double transit probability is at a maximum. Rearranging equation (20) one finds

$$\begin{aligned} \Delta i_{\rm crit} &\approx \frac{R_\star/a_1 - R_\star/a_2}{2K_{\rm simp}} \quad \text{for } K_{\rm simp} < 1 \\ &\approx \frac{R_\star/a_1 - R_\star/a_2}{2} \quad \text{otherwise,} \end{aligned} \tag{21}$$

where $\Delta i_{\rm crit}$ is the inclination of the non-transiting planet required to significantly reduce the mean probability that the inner planets are observed to transit due to secular interactions. We note that equation (21) assumes that the transiting planets are initially coplanar. However, if these planets were initially mutually inclined by a small amount, a smaller secular perturbation from the outer planet would be required to significantly reduce the mean probability that the inner planets are observed to transit. In this case, $i_{\rm crit}$ from equation (21) would be reduced.

5.1 Kepler-56

Kepler-56 is a red giant star with a mass and radius of 1.32 ± 0.13 $M_\odot$ and 4.23 ± 0.15 $R_\odot$, respectively (Huber et al. 2013), which is observed to host three planets. Interestingly, Kepler-56 represents one of the few red giant stars observed to host a planetary system (Lillo-Box et al. 2014; Ciceri et al. 2015; Quinn et al. 2015; Pepper et al. 2016). The two inner planets (b, c) are observed to transit with periods of 10.5 and 21.4 d, respectively (Borucki et al. 2011; Steffen et al. 2013; Huber et al. 2013; Hadden & Lithwick 2014; Holczer et al. 2016; Morton et al. 2016) and have masses of $22.1^{+3.9}_{-3.6}$ and 181^{+21}_{-19} $M_\oplus$, respectively (Huber et al. 2013). Keck/HIRES and HARPS-North observations have revealed a non-transiting giant planet (d) with a period of 1002 ± 5 d and minimum mass of $5.62 \pm 0.38 M_J$ (Huber et al. 2013; Otor et al. 2016). An interesting quirk of this system is that the transiting planets, while being roughly coplanar, are misaligned to the stellar spin axis by $\sim 40^\circ$ (Huber et al. 2013). It is unclear if this large obliquity is caused by long-term dynamical interactions with a highly inclined companion, such as Kepler-56d, or from the star being inherently tilted to the disc from which the planets formed (Li et al. 2014).

Applying equation (21), we find that $i_{\rm crit} = 704^\circ$. This unphysically large value means that, regardless of how Kepler-56d is inclined in this system, the mean double transit probability of the inner two transiting planets cannot be significantly reduced. That is, we suggest that the transiting planets in Kepler-56 are not strongly affected by the secular perturbations of Kepler-56d, regardless of its mutual inclination. This is a similar result to that found in Lai & Pu (2017), who also find that the inner planets are strongly coupled against external secular interactions. We therefore cannot place any constraint on the inclination of Kepler-56d using this method. We note, however, that this does not preclude that the 40° misalignment from the stellar spin axis comes from an inclined outer companion, since both inner planets could be inclined together without significant mutual inclination.

5.2 Kepler-68

Kepler-68 is a roughly solar type star with a mass and radius of 1.08 ± 0.05 $M_\odot$ and 1.24 ± 0.02 $R_\odot$, respectively (Gilliland et al. 2013; Marcy et al. 2014). It hosts two transiting planets (b, c) with periods of 5.4 and 9.6 d, respectively (Gilliland et al. 2013; Marcy et al. 2014; Van Eylen & Albrecht 2015; Holczer et al. 2016; Morton et al. 2016) and fitted masses of 5.97 ± 1.70 and 2.18 ± 3.5 $M_\oplus$, respectively (Marcy et al. 2014). Keck/HIRES RV follow-up of this system detected a non-transiting planet (d) with a period of 625 ± 16 d with a fitted mass of 267 ± 16 $M_\oplus$ (Marcy et al. 2014).

Applying equation (21), we find $i_{\rm crit} = 244^\circ$. Similar to Kepler-56 therefore, regardless of the mutual inclination of Kepler-68d, the mean double transit probability of the inner two transiting planets cannot be significantly reduced by secular perturbations. We therefore cannot place a constraint on the inclination of Kepler-68d using this method. We note that Kepler-68d can indeed have a large inclination without affecting the overall stability of the system according to a suite of N-body simulations, which suggests that Kepler-68d is inclined by $\Delta i < 85^\circ$ (Kane 2015).

5.3 HD 106315

HD 106315 is a bright F dwarf star at a distance $d = 107.3 \pm 3.9$ pc (Gaia Collaboration et al. 2016) with a mass and radius of

$1.07 \pm 0.03\ M_\odot$ and $1.18 \pm 0.11\ R_\odot$, respectively (Morton 2012; Petigura 2015; Crossfield et al. 2017). Recent *K2* observations detect two transiting planets (b, c) with periods of 9.55 and 21.06 d, respectively, and radii of $2.23^{+0.30}_{-0.25}$ and $3.95^{+0.42}_{-0.39}\ R_\oplus$, respectively (Crossfield et al. 2017; Rodriguez et al. 2017). Mass–radius relationships suggest that these planets have masses of 8 and 20 $M_\oplus$, respectively (Weiss et al. 2016; Wolfgang, Rogers & Ford 2016; Crossfield et al. 2017). Further Keck/HIRES RV observations also indicate the presence of a third outer companion planet (d) with a period of $P_d \gtrsim 80$ d, which has a mass of $m_d \gtrsim 1 M_J$ (Crossfield et al. 2017). As the exact period of this outer planet is unknown, we consider two possibilities where the outer planet has a period of $P_d = 80$ and 365 d, respectively. Assuming $P_d = 80$ d implies a mass of $m_d = 1 M_J$ (Winn et al. 2009; Crossfield et al. 2017). Applying equation (21) with this outer planet gives $i_{crit} = 1.^\circ1$. This suggests that if the outer planet had a period of $P_d = 80$ d, it must have an inclination of $\Delta i \lesssim 1.^\circ1$; otherwise, the mean probability of observing the inner two planets to transit would be significantly reduced due to the secular interaction. Conversely, if the outer planet is assumed to be farther out with $P_d = 365$ d, implying a mass of $\sim 7 M_J$, equation (21) suggests that $i_{crit} = 2.^\circ4$. That is, if the outer planet has a period of $P_d = 365$ d, it must have an inclination of $\Delta i \lesssim 2.^\circ4$; otherwise, the secular interaction would significantly reduce the mean probability that the inner planets are observed to transit.

The mutual inclination of the outer planet might also be constrained through astrometric observations of HD 106315 with ESA's *Gaia* mission (Perryman et al. 2001; Casertano et al. 2008; Perryman et al. 2014; Sozzetti et al. 2014; Sahlmann, Triaud & Martin 2015). The astrometric displacement of the host star due to the presence of a planet is defined by

$$\alpha = \left(\frac{m_p}{M_\star}\right)\left(\frac{a_p}{1\ \mathrm{au}}\right)\left(\frac{d}{1\ \mathrm{pc}}\right)^{-1} \mathrm{arcsec}, \tag{22}$$

with the astrometric signal-to-noise ratio equal to $S/N = \alpha\sqrt{N_{obs}}/\sigma$, where N_{obs} is the scheduled number of astrometric measurements ($N_{obs} = 36$ for HD 106315[2]) with typical uncertainties of $\sigma = 40\ \mu$as (de Bruijne 2012). If $S/N > 20$, the orbital inclination can be constrained to a precision of $<10^\circ$ (Sahlmann et al. 2015). We find that for the example periods and masses considered above for HD 106315d $S/N < 10$. We therefore expect that the inclination of the above examples of HD 106315d cannot be constrained using *Gaia* astrometry. However, if HD 106315d is outside of $\sim$1.3 au, (implying a mass of $\gtrsim 12 M_J$) equation (22) suggests that $S/N > 20$ such that the inclination of HD 106315d should be constrained by *Gaia* astrometry. Further RV follow-up of this system will allow for greater constraints to be placed on the mass and the orbit of HD 106315d, which, in turn, allow for greater constraints to be placed on the inclination, either through potential astrometry measurements or through our model represented by equation (21).

5.4 Systems with three transiting planets and a wide-orbit companion

Here we generalize the effect a wide-orbit planet has on the transit probabilities of three inner transiting planets. Consider Kepler-48 as an example of such a system. Kepler-48 has a mass and radius of $M_* = 0.88 \pm 0.06\ M_\odot$ and $R_* = 0.89 \pm 0.05\ R_\odot$, respectively. It hosts three transiting planets (b, c and d) with periods of 4.78, 9.67 and 42.9 d and fitted masses of 3.94 ± 2.10, 14.61 ± 2.30 and $7.93 \pm 4.6\ M_\oplus$ (Steffen et al. 2013; Hadden & Lithwick 2014; Marcy et al. 2014; Holczer et al. 2016; Morton et al. 2016). Keck/HIRES RV analysis also detects a non-transiting planet (e) with a period and fitted mass of 982 ± 8 d and $657 \pm 25\ M_\oplus$, respectively (Marcy et al. 2014).

[2] http://gaia.esac.esa.int/gost/

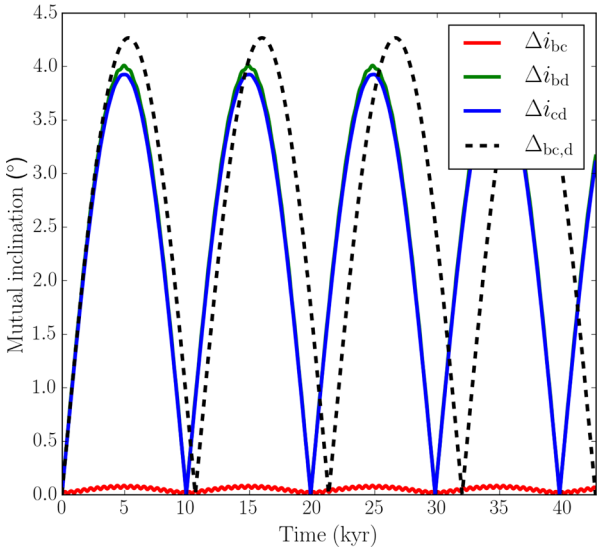

Figure 7. The mutual inclination between the respective planets in Kepler-48, when the non-transiting planet, Kepler-48e, is initially mutually inclined by $\Delta i = 10^\circ$. The black dashed line shows the evolution of the mutual inclination between the inner two transiting planets with the outer transiting planet, for when the inner two planets are treated as a single body with an equal orbital angular momentum.

Returning to the derivation of the secular interaction in Section 3, the initial inclination of the non-transiting planet, i_e, with respect to the invariable plane can be generalized to

$$i_e = \arctan\left(\frac{\sin\Delta i\left(\sum_{n=1}^{3} L_n\right)}{L_e + \cos\Delta i\left(\sum_{n=1}^{3} L_n\right)}\right), \tag{23}$$

where $L_e = m_e a_e^{1/2}$ and is proportional to the angular momentum of Kepler-48e in the low eccentricity limit and $L_n = m_n a_n^{1/2}$ for either Kepler-48b, c or d. The initial inclination of the transiting planets is therefore equal to $\Delta i - i_e$.

As the strength of the secular interaction between planets largely depends on their separation (e.g. equation 19), we assume that Kepler-48d will be affected most by perturbations from the non-transiting planet. We demonstrate this in Fig. 7, which shows how the mutual inclination between each of the transiting planets evolves assuming Laplace–Lagrange theory (equation 11) and that Kepler-48e is initially mutually inclined by $\Delta i = 10^\circ$. The red line shows the mutual inclination between Kepler-48b and Kepler-48c (Δi_{bc}), the blue between b and d (Δi_{bd}) and the green between c and d (Δi_{cd}). The mutual inclination between Kepler-48b and Kepler-48c is largely unchanged, and they remain roughly coplanar. Conversely, the mutual inclination between b and d and c and d is significant and roughly equal throughout the secular evolution. It can be assumed for Kepler-48 therefore that the inner two transiting planets are largely unaffected by the secular perturbations of Kepler-48e,

but both can become significantly mutually inclined to the outer transiting planet.

As such, we assume that Kepler-48b and c can be treated as a single body whose angular momentum is the sum of Kepler48-b and c, reducing the system to a total of three planets. With this approximation, the evolution of the mutual inclination between Kepler-48b and c with d ($\Delta i_{\rm bc,\,d}$) is shown by the dashed black line in Fig. 7. It can be seen that this way of treating Kepler-48b and c as a single body gives a good approximation for the evolution of the mutual inclination between Kepler-48b and c with d.

The initial mutual inclination of Kepler-48e, which causes a significant reduction in the mean probability of the inner planets transiting, $\Delta i_{\rm crit}$, can therefore be approximated by equation (21), where the value of $K_{\rm simp}$ becomes

$$K_{\rm simp} = \frac{3 m_{\rm e} a_{\rm d}^{7/2}}{m_{\rm d} a_{\rm bc}^{1/2} a_{\rm e}^{3}} \frac{1}{b^{1}_{3/2}\left(\frac{a_{\rm bc}}{a_{\rm d}}\right)\left(1+(L_{\rm bc}/L_{\rm d})\right)}, \tag{24}$$

with the subscripts referring to the respective planets and the subscript 'bc' to the planet that has the same total angular momentum as Kepler-48b and c.

We find that $\Delta i_{\rm crit} = 3.^{\circ}7$. This suggests therefore that the inclination of Kepler-48e is $\Delta i \lesssim 3.^{\circ}7$; otherwise, the secular interaction would cause a significant reduction in the mean probability that all three inner planets are observed to transit. Under the simpler assumption that $\max|\Delta i_{\rm bc,\,d}| \lesssim R_*/a_{\rm d}$, Lai & Pu (2017) also find that the inclination of Kepler-48e, considering secular interactions only, must also be small with $\Delta i \lesssim 2.^{\circ}3$.

6 APPLICATION TO THE KEPLER DICHOTOMY

As discussed in Section 1, *Kepler* has observed an excess of single transiting systems, which cannot be explained by geometric effects alone, commonly referred to as the Kepler Dichotomy (Lissauer et al. 2011; Youdin 2011; Johansen et al. 2012; Ballard & Johnson 2016). This may suggest that there is a population of inherently single transiting systems in addition to a population of multiplanet systems with small inclination dispersions. However, there may also be a population of multiplanet systems where the mutual inclination dispersion is large, increasing the probability that only a single planet is observed to transit. Here we investigate whether both these types of multiplanet systems can significantly contribute to the abundance of systems observed by *Kepler* to have one and two transiting planets, respectively.

The *Kepler* systems we consider are discussed in Section 6.1. A method for debiasing *Kepler* systems to a general population of planetary systems is described in Section 6.2. We consider the scenario where planets share some inherently fixed mutual inclination in Section 6.3, before considering when this mutual inclination is evolving due to the presence of an outer inclined planetary companion in Section 6.4. We note from the outset that we do not consider *Kepler* systems observed to have more than two planets. Instead, we look to explore what effects an outer planet might have on observables of a subset of *Kepler*-like systems, rather than observables of the whole *Kepler* population. We discuss this assumption further in Section 7.6.

6.1 *Kepler* candidate sample

We select planet candidates from the cumulative *Kepler* objects of interest (KOIs) table from the NASA exoplanet archive,[3] accessed on 2016 September 13. The vast majority of the KOIs (∼97 per cent) that survive our cuts detailed below, to make it into our final sample, are listed as being taken from the most recent Q1-17 DR24 data release. This data release is of particular note as it incorporates an automated processing of all KOIs (Coughlin et al. 2016).

Out of the initial 8826 KOIs, we consider those that orbit solar-type stars, with surface temperatures and surface gravities in the range $4200 < T < 7000$ K and $4.0 < \log(g) < 4.9$, respectively. This reduces the total number of KOIs to 7446. We also find that the total number of unique *Kepler* stars within this range (discussed in Section 7) is 164 966 from the 'Kepler Stellar data' table. We next remove false positives, which refer to KOI light curves that are indicative of either an eclipsing binary, having significant contamination from a background eclipsing binary, showing a significant stellar variability that mimics a planetary transit, or where instrument artefacts have produced a transit-like signal (see Coughlin et al. 2014; Rowe et al. 2014, 2015; Seader et al. 2015; Coughlin et al. 2016). This reduces our sample of KOIs (hereafter candidates) to 4072 objects. We subsequently remove non-planetary-like objects with radii >22.4 $R_\oplus$ (Borucki et al. 2011), leaving 3757 objects, after which we remove candidates with an S/N <10, reducing the possibility that a transit signal is caused by systematic background noise (Morton et al. 2016), leaving 3327 objects. Finally, we remove candidates listed as not having a satisfactory fit to the transit signal (Rowe et al. 2014, 2015). This gives our final sample of 3255 objects. We note that our choice of cuts means that KOI systems can become reduced in multiplicity. We find that our final sample includes systems that contain one to six candidates with $N_i = (1, 2, 3, 4, 5, 6) = (1951, 341, 117, 43, 15, 4)$, for example, 1951 systems with a single candidate, 341 systems with two candidates, and so on. Herein, we consider the 1951 systems observed by *Kepler* to have a single transiting planet and the 341 systems observed to have two.

The smoothed distribution of the semi-major axes and planetary radii for the single and double planet transiting systems is shown in Fig. 8. Comparing the left- and right-hand panels of Fig. 8, there are types of planets that are present only in single transiting systems. We briefly discuss these differences here for future reference. Large planets with short periods, i.e. hot Jupiters, are not present in *Kepler* systems with two transiting planets. Indeed, investigations into the formation processes of hot Jupiters predict a lack of close companions (Wright et al. 2009; Steffen et al. 2012; Mustill, Davies & Johansen 2015; Huang, Petrovich & Deibert 2016, see WASP-47 for an exception, Becker et al. 2015; Almenara et al. 2016). Long-period planets are also more abundant in the population of single transiting systems. This may not necessarily indicate that long-period planets inherently favour being in single transiting systems, but instead they might be the inner planet of a higher multiplicity system where the outer planets are on too long a period to produce a significant transit signal.

Finally, there appears to be an overabundance in the population of single transiting systems for planets with $R_{\rm p} \lesssim 2\,R_\oplus$ at periods $P < 10$ d ($\lesssim$0.03 au) (see Lissauer et al. 2011; Johansen et al. 2012; Lopez & Rice 2016; Steffen & Coughlin 2016). The formation processes that lead to these types of planets are unclear.

[3] exoplanetarchive.ipac.caltech.edu

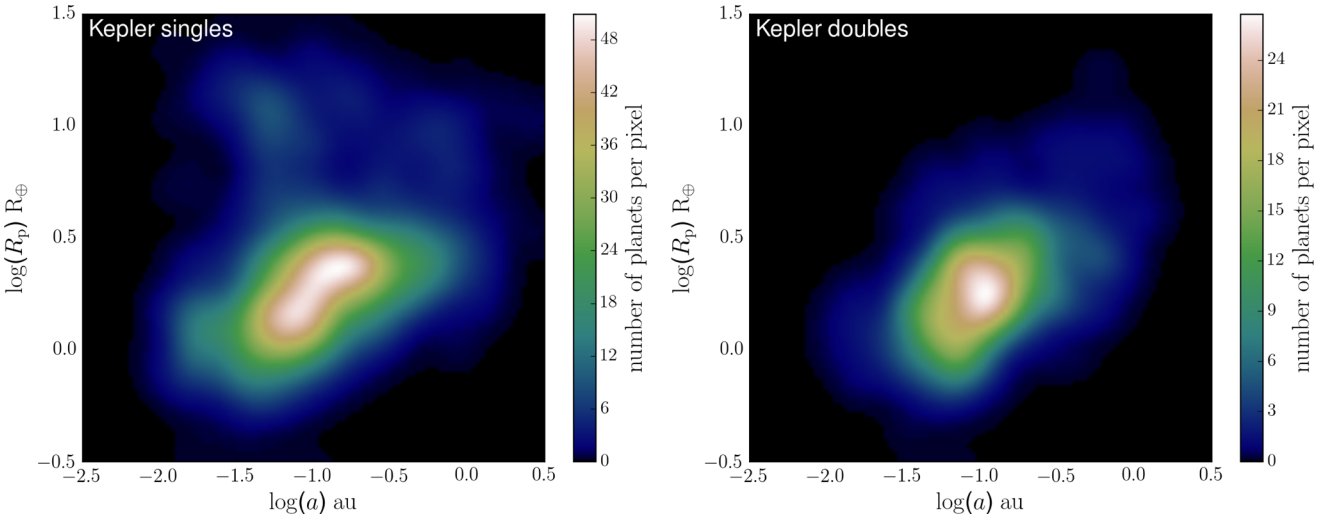

Figure 8. The smoothed distribution of the radii and the semi-major axes of planets observed by *Kepler* to be in systems with a single transiting planet (left-hand panel) and in systems with two transiting planets (right-hand panel). Pixel sizes are $\log(a) = 0.15$ by $\log(R_\mathrm{p}) = 0.1$.

It is also unknown if these objects are inherently rocky planets, or are the cores of Neptune-sized planets whose envelopes have been irradiated (Dressing & Charbonneau 2015; Rogers 2015; Lopez & Rice 2016). If these outlying systems are largely ignored, the question remains of whether the remaining planets in single transiting systems are part of the same underlying distribution of higher order planetary systems; i.e. could these single transiting systems contain similar planets that are not observed to transit?

For our dynamical analysis, it is not the radii of these planets that are of relevance, rather their masses. We estimate the masses of planets according to the following mass–radius relations. For radii less than 1.5 $\mathrm{R}_\oplus$, we use the rocky planet mass–radius relation from Weiss & Marcy (2014), where density (ρ_p) is related to radii (R_p) through $\rho_\mathrm{p} = 2.43 + 3.39(R_\mathrm{p}/\mathrm{R}_\oplus)\mathrm{g\,cm}^{-3}$. For radii $1.5 \leq R_\mathrm{p} \leq 4\,\mathrm{R}_\oplus$, we use the deterministic version of the probabilistic mass–radius relation for sub-Neptune objects from Wolfgang et al. (2016), where mass (M_p) is given by $M_\mathrm{p}/\mathrm{M}_\oplus = 2.7(R_\mathrm{p}/\mathrm{R}_\oplus)^{1.3}$. Once radii become $R_\mathrm{p} \gtrsim 4\ \mathrm{R}_\oplus$, deterministic mass–radius relations become uncertain due to the onset of planetary contraction under self-gravity (see Chen & Kipping 2017). From the mass–radius relations detailed in Chen & Kipping (2017), we find that their 'Neptunian worlds' deterministic relation of $M_\mathrm{p}/\mathrm{M}_\oplus = (1.23R_\mathrm{p}/\mathrm{R}_\oplus)^{1.7}$ gives the most sensible masses for all planets with $R_\mathrm{p} > 4\,\mathrm{R}_\oplus$.

6.2 Debiasing the *Kepler* population

As previously alluded to, *Kepler* only observes planetary systems that have their orbital planes aligned with our line of sight. It is therefore sensible to suggest that there is a much larger, underlying population of planetary systems within which only some are observed to transit. We refer to this underlying population of planetary systems as the *model population*. Conversely, we refer to the population of planetary systems actually observed by *Kepler* as the *Kepler population*. We assume that *Kepler* systems are representative of planetary systems in the model population once geometrical biases have been taken into account.

To construct an underlying model population, our primary goal is for this to predict the correct number and planet parameter distribution seen in the *Kepler* population for systems with two transiting planets (Fig. 8, right-hand panel). To achieve this, we first assume that all stars either have two or zero planet. Any system that hosts two planets is assumed to be identical to one of the 341 double transiting systems observed by *Kepler*. We assume that the abundance of a specific *Kepler*-like system in the model population is equal to the inverse of the mean of the double transit probability calculated by the method outlined in Section 2. Systems with inherently low mean double transit probabilities are therefore probabilistically assumed to be more numerous in the model population. By definition therefore, each unique system in the model population would be expected to be observed with both planets transiting exactly once, and so the model population predicts the correct distribution shown in the right-hand panel of Fig. 8. We note that a model population generated in this way is similar to the method described in Johansen et al. (2012), albeit with their work predicting the correct number and planet parameter distribution seen in the *Kepler* population for systems with three transiting planets.

The sum of the inversed mean double transit probabilities of all the 341 double transiting systems gives the total number of planetary systems in the model population. If we assume that all of the two-planet systems are coplanar, we find that the model population includes 16 517 systems (the remaining 148 449 systems observed by *Kepler* are assumed to have no planets).

Each system in the model population can be observed to have a single transiting planet, depending on the viewing angle. The sum of the mean single transit probabilities for each of the 16 517 systems in the coplanar model population gives the total number of single transiting planets, N_sing, that would be expected to be observed. Here the mean single transit probability for a given system is equal to $R_*/a_1 - R_*/a_2$, where a_1 and a_2 are the semi-major axes of each planet when $a_2 > a_1$ and R_* is the radius of the host star. We find $N_\mathrm{sing} = 589$, which clearly underestimates the 1951 single transiting systems in the observed *Kepler* population, by a factor of $\sim$3. This is the Kepler Dichotomy discussed in Section 1. We show the smoothed distribution of the semi-major axes and planet radii for these 589 predicted single transiting planets in the top left-hand panel of Fig. 9, which when compared with the left-hand panel of Fig. 8 clearly shows an underprediction of the single transiting planets observed by *Kepler*.

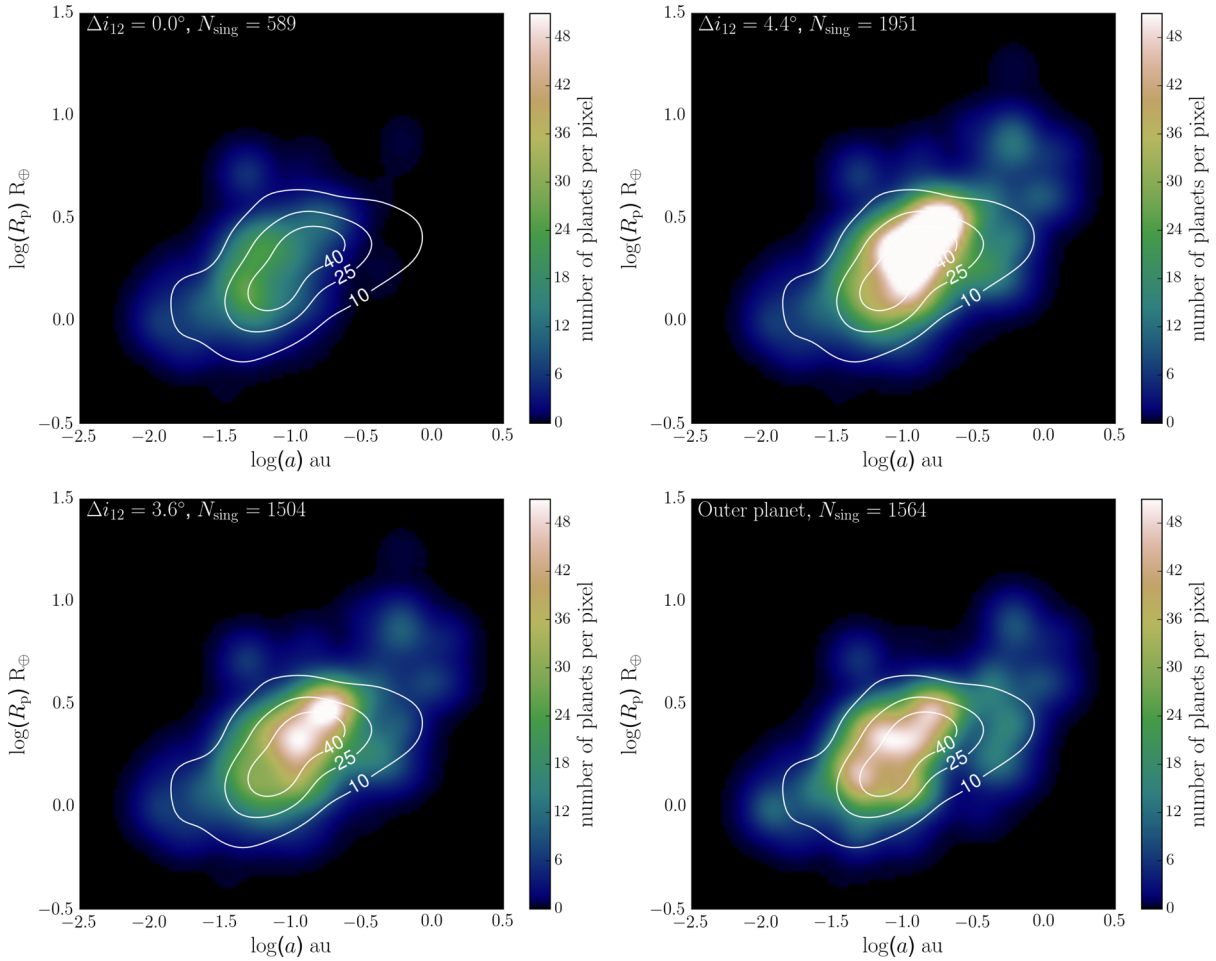

Figure 9. The distribution of the radii and semi-major axes of single transiting planets observed from the model population with (top) no third planet. Middle: a third planet with $m_3 = 1 M_{\rm J}$, $a_3 = 1.9$ au and $\Delta i = 10°$. The total number of single transiting planets predicted by the model population is equal to that observed by *Kepler*. The colour scale for this panel is saturated for ease of comparison. Bottom: a third planet with $m_3 = 24$ M$_\oplus$, $a_3 = 1.07$ au and $\Delta i = 10°$. We find that the 1564 single transiting planets predicted here are a best fit to those observed by *Kepler* (left-hand panel of Fig. 8). The contours show the distribution of single transiting planets from the *Kepler* population. Pixel sizes are $\log(a) = 0.15$ by $\log(R_{\rm p}) = 0.1$.

6.3 Inherently inclined multiplanet systems

From transit duration variation (TDV) studies, the mutual inclinations of planets in multitransiting systems are small in the range $\lesssim 2°$–$3°$ (Fang & Margot 2012; Fabrycky et al. 2014). We note that this mutual inclination also best fits the distribution of impact parameters in the *Kepler* population. Perhaps then, if two planets are assumed to be inherently mutually inclined by a small amount, this may account for the abundance of single transiting planets in the *Kepler* population. Consider a fixed mutual inclination Δi_{12} between the two planets in each of the 341 double transiting systems. The mean single transit probability for each planet from a given system, $P_{\rm sing,\,1}$ and $P_{\rm sing,\,2}$, respectively, where $P_{\rm sing,\,1} > P_{\rm sing,\,2}$, is now given by

$$P_{\rm sing,1} = \frac{R_\star}{a_1} - P,$$
$$P_{\rm sing,2} = \frac{R_\star}{a_2} - P, \qquad (25)$$

where P is the mean double transit probability and $P_{\rm sing,\,1} + P_{\rm sing,\,2}$ is the total mean single transit probability for this system. As Δi_{12} increases, the mean double transit probability decreases (Fig. 3). Therefore, for a fixed population of double transiting systems considered here, the expected abundance of single transiting systems increases. Fig. 10 shows how $N_{\rm sing}$ increases with Δi_{12} for when the number of double transiting systems is kept constant at 341 systems. If $\Delta i_{12} = 4.^\circ4$, we find $N_{\rm sing} = 1951$, i.e. the number of single transiting planets expected to be observed from the model population is equal to the number in the observed *Kepler* population. This suggests that mutual inclinations in *Kepler* systems observed with two planets must be less than $4.^\circ4$, or the number of single planet systems observed by *Kepler* would be too large relative to the number of doubles.

We show the distribution of the semi-major axes and radii of the expected single transiting planets for when $\Delta i = 4.^\circ4$ in the top right-hand panel of Fig. 9. Comparing with the left-hand panel of Fig. 8, there is an overabundance of predicted single transiting planets with radii of ~ 2.5 R$_\oplus$ and semi-major axes of ~ 0.15 au. This is due to the model population compensating for not being able to reproduce all types of single transiting planets in the *Kepler* population (e.g. hot Jupiters discussed in Section 6.1). Herein therefore when discussing how well a model population predicts the *Kepler* population of single transiting planets, we refer to how well the *types* of planets from each population compare, rather than the total number. That

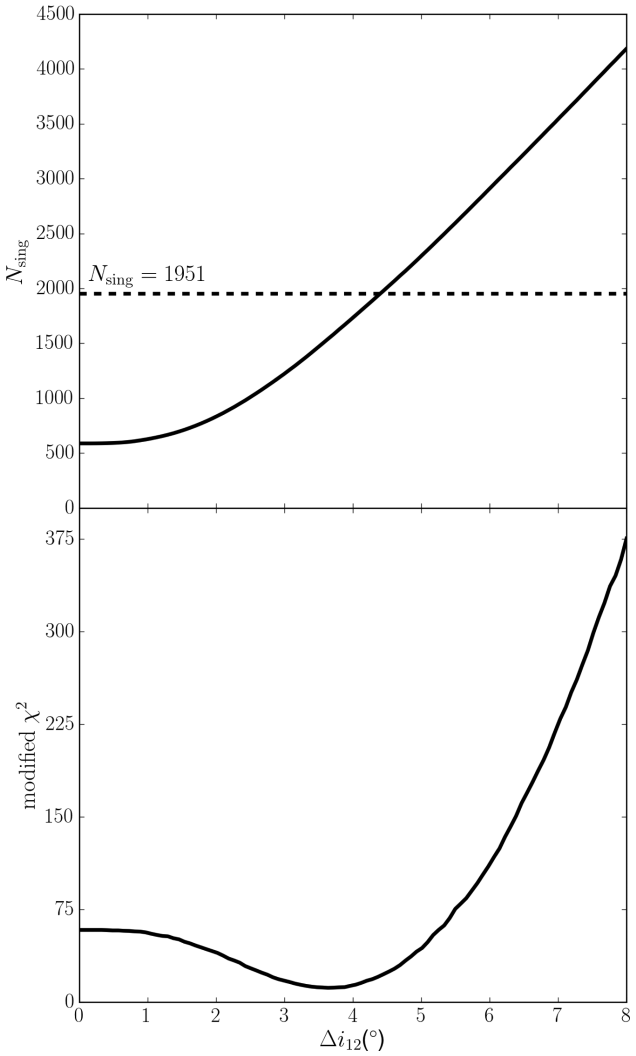

Figure 10. Top panel: the expected number of single transiting planets observed from a model population generated from *Kepler* systems with two planets that are mutually inclined by Δi_{12}. The number of double transiting systems predicted by the model population is constant with 341 systems. Bottom panel: the associated modified χ^2 comparing types of single transiting planets predicted by the model population with the *Kepler* population. The minimum modified χ^2 value corresponds to $\Delta i_{12} = 3.^\circ 6$.

is, we look to find which value of Δi_{12} causes the associated version of the top right-hand panel of Fig. 9 to be most like the left-hand panel of Fig. 8.

We judge the success of this comparison using a modified χ^2 minimization test, in which we simply sum the square of the difference between the number of singles with a given radius and semi-major axis expected from the model population, with that of the observed *Kepler* population. Varying Δi_{12} we therefore look to identify a minimum in the modified χ^2 space without caring for the modified χ^2 value itself. We show this in Fig. 10, with the modified χ^2 minimum occurring for $\Delta i_{12} = 3.^\circ 6$. The distribution of the single transiting planets expected from the model population for this mutual inclination is shown in the bottom left-hand panel of Fig. 9. Comparing with the left-hand panel of Fig. 8, these single transiting planets share a stronger agreement with those in the *Kepler* population, compared with when the outer planet predicted $N_{\rm sing} = 1951$ (e.g. top right-hand panel of Fig. 9). We note that the total number of single transiting planets expected from the model population for $\Delta i_{12} = 3.^\circ 6$ is 1504. We assume therefore that the remaining $1951 - 1504 = 447$ single transiting transiting planets in the *Kepler* population not fitted by this model population are *inherently single planet systems*.

Despite the model population for $\Delta i_{12} = 3.^\circ 6$ giving the lowest modified χ^2 value, this mutual inclination is perhaps larger than that suggested by TDV studies. We note, however, that mutual inclination estimates from TDV studies consider a range of planet multiplicities. For example, Fang & Margot (2012) consider a model population of planetary systems with one to seven or more planets and predict that ∼50 per cent of observed planetary systems should contain a single planet, with the remaining systems containing multiple planets with mutual inclinations of $\lesssim 3^\circ$. In order to properly predict the inherent mutual inclination in the multiplanet systems considered in this work, therefore, it would be necessary to simultaneously model the TDV data directly. We consider such an analysis as part of future work. Instead, in Section 6.4, we consider the possibility that *Kepler* planets form coplanar, but end up mutually inclined due to perturbations from an outer planetary companion on an inclined orbit. This may provide another way to predict the correct abundance of single transiting systems observed by *Kepler*, and also result in a low mutual inclination for those systems with two transiting planets.

6.4 Including an inclined planetary companion

We now consider the effects of a hypothetical outer planet in each of the systems in the model population. We first amend the assumption from Section 6.2 and assume that all stars either host three or zero planet. Any system that hosts three planets is assumed to be identical to one of the 341 double transiting systems from the *Kepler* population plus an additional outer planet. The outer planet is assumed to have the same mass and semi-major axis in all systems and starts on an inclination to the inner planets when these are coplanar, causing the mutual inclination between the inner planets to evolve according to equation (15). We assume that the outer planet satisfies the Hill stability criterion of $\Delta = 2\sqrt{3}$ (Chambers 1999) with the outer of the inner two planets for all 341 considered systems, where $\Delta = (a_3 - a_2)/R_{\rm H}$ and

$$R_{\rm H} = \left(\frac{m_2 + m_3}{3M_\star}\right)^{1/3} \left(\frac{a_2 + a_3}{2}\right),$$

where M_* is the stellar mass. If this criterion is not satisfied, we move the outer planet for this specific system until it is. For example, when the outer planet is assumed to have a semi-major axis and mass of 1 au and 1 $M_\oplus$, respectively, we find that 6 of the 341 systems do not satisfy this stability criterion and the outer planet needs to be moved to a mean semi-major axis of 1.2 au. When the outer planet has a semi-major axis and mass of 1 au and $10M_{\rm J}$, respectively, we find that 22 of the 341 systems do not satisfy the stability criterion and the outer planet needs to be moved to a mean semi-major axis of 1.4 au.

Each one of the 341 systems is again replicated enough times in the model population to be expected to be observed exactly once. That is, the inverse of the mean double transit probability of the inner two planets gives the abundance of each of the 341 systems in the model population. The associated mean single transit probability for each of the inner two planets is of the same form as equation (25). The sum of the mean single transit probabilities for every system in the model population therefore again gives the abundance of a given single transiting planet that would be expected to be observed from

the model population that also fits the number of double transiting systems.

Similarly to the modelling approach in Section 6.3, we look to identify which mass (m_3), semi-major axis (a_3) and initial inclination (Δi) of the outer planet cause the types of single transiting systems expected from the associated model population to be most like those in the observed *Kepler* population. For a given combination of a_3, m_3 and Δi, we therefore calculate a modified χ^2 value described in Section 6.3. We show these modified χ^2 values in Fig. 11 for an outer planet with $\Delta i = 10^\circ$ (top panel), $m_3 = 1 M_J$ (middle panel) and $a_3 = 2$ au (bottom panel). Inclinations of $\Delta i \gg 20^\circ$ where equation (15) is expected to break down are included for completeness.

From the top panel in Fig. 11, it is clear that there is a 'valley' of semi-major axes and masses of the outer planet that causes a significantly lower modified χ^2 value. It can be assumed therefore that such an additional planet predicts single transiting systems whose radii and semi-major axes better fit those in the *Kepler* population. However, there is also a distinct minimum in the modified χ^2 space when the outer planet has a semi-major axis of $\sim$1 au for a mass of $\sim$30 $M_\oplus$. Similarly, in the other panels of Fig. 11, there appear to be distinct minima. For the middle panel, this occurs for an outer planet (of $m_3 = 1 M_J$) with a semi-major axis of 1.38 au, initially inclined to the inner planets by $\Delta i = 5.^\circ 7$. Finally, for the bottom panel, this minimum occurs for a mass of $\sim 6 M_J$ and inclination of 6° (where $a_3 = 2$ au). Generally, we find that the distribution of single transiting planets expected from the model population is more representative of those in the *Kepler* population for $3^\circ \lesssim \Delta i \lesssim 10^\circ$.

The bottom right-hand panel of Fig. 9 gives the distribution of single transiting planets expected from the model population when the outer planet exists in a minimum of the modified χ^2 space with $a_3 = 1.07$ au, $m_3 = 24$ $M_\oplus$ and $\Delta i = 10^\circ$ (white circle in the top panel of Fig. 11). We note that the total number of single transiting planets expected from this model population is 1564. The outer planet parameters that predict $N_{\rm sing} = 1564$ are shown by the white lines in Fig. 11. This line highlights that while many outer planet parameters can predict $N_{\rm sing} = 1564$, some predict single transiting planets that are more representative of those in the *Kepler* population. We note that $N_{\rm sing}$ predicted by the same range of outer planet parameters from Fig. 11 is shown in Appendix C.

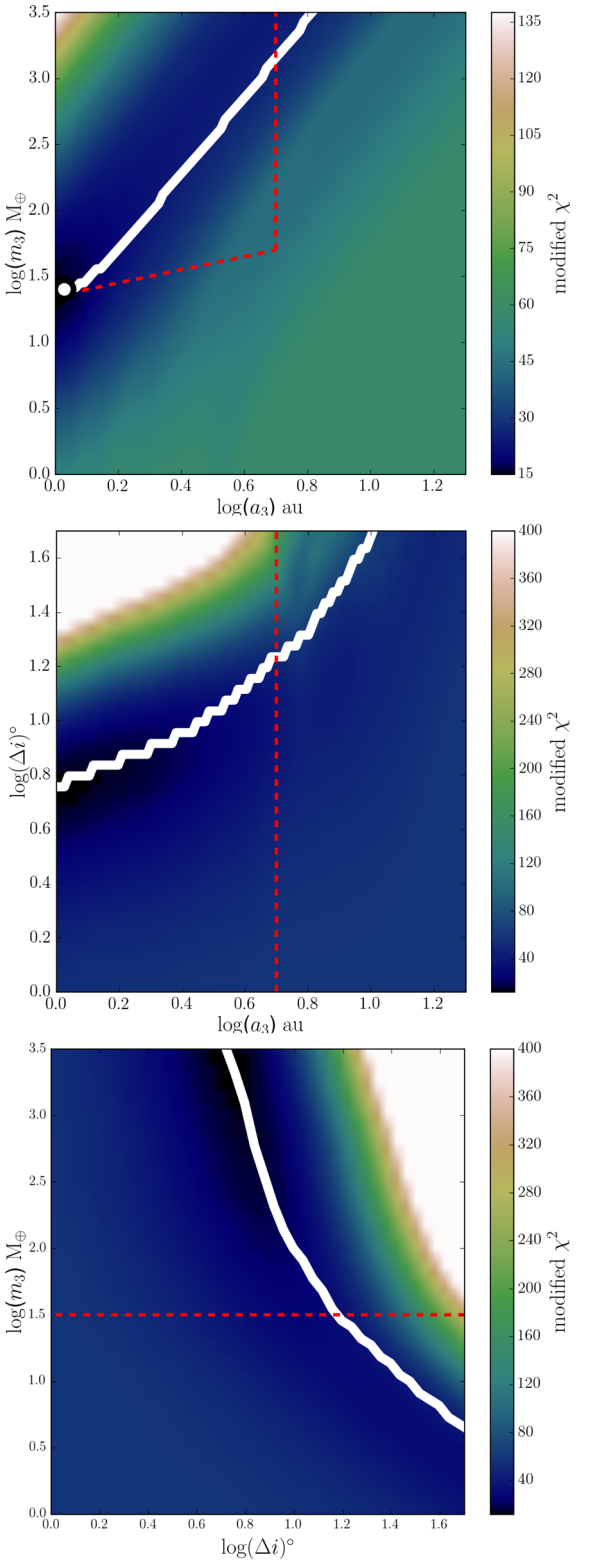

Figure 11. Modified χ^2 value comparing types of single transiting planets predicted by the model with the *Kepler* population. For the top panel, $\Delta i = 10^\circ$, for the middle panel, $m_3 = 1 M_J$, and for the bottom panel, $a_3 = 2$ au. Laplace–Lagrange theory is expected to break down for $\Delta i \gg 20^\circ$. The red dashed line refers to a rough RV detection threshold. The white line shows where the model population predicts $N_{\rm sing} = 1564$. The white triangle and circle give the third planet parameters used to produce the middle and bottom panels of Fig. 9, respectively.

7 DISCUSSION

7.1 Combining inherently mutually inclined and outer planet populations

In reality, it is likely that the total number of single planet transiting systems observed by *Kepler* ($N_{\rm sing,\,Kep} = 1951$) is contributed to by different populations of planetary systems. These may include a number of inherently single planet systems ($N_{\rm sing,\,inh}$) in addition to a number of single transiting planets observed from a population of two-planet systems that have a fixed mutual inclination of Δi_{12} ($N_{{\rm sing},\,\Delta i_{12}}$). They may also include a number of single transiting planets that are observed from a population of initially coplanar two-planet systems interacting with an inclined planetary companion ($N_{\rm sing,\,planet}$). Hence, in general, it can be considered that

$$N_{\rm sing,Kep} = N_{\rm sing,inh} + N_{{\rm sing},\Delta i_{12}} + N_{\rm sing,planet}. \quad (26)$$

Here we make the assumption that the total number of double transiting systems observed by *Kepler* ($N_{\rm doub,\,Kep} = 341$) is made up of a fraction f that are two-planet systems with an inherent mutual

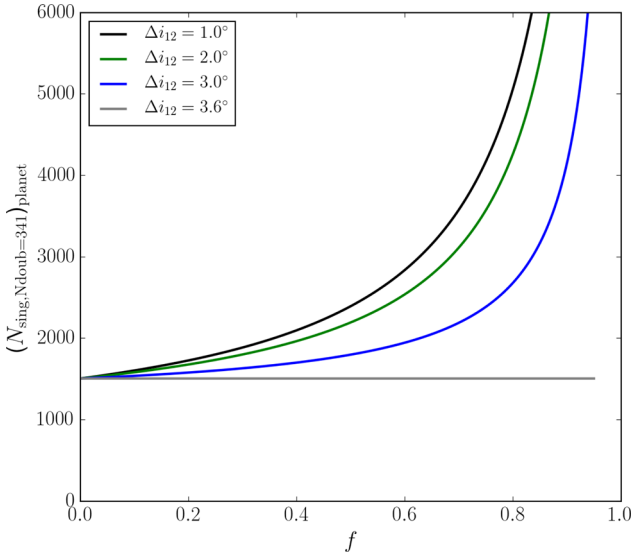

Figure 12. The number of single transiting planets needed to be predicted by a population of two-planet systems with an outer planetary companion, assuming that $(1 - f)$ of observed *Kepler* systems host such systems. The remaining fraction of observed *Kepler* systems are assumed to be two-planet systems inherently mutually inclined by Δi_{12}.

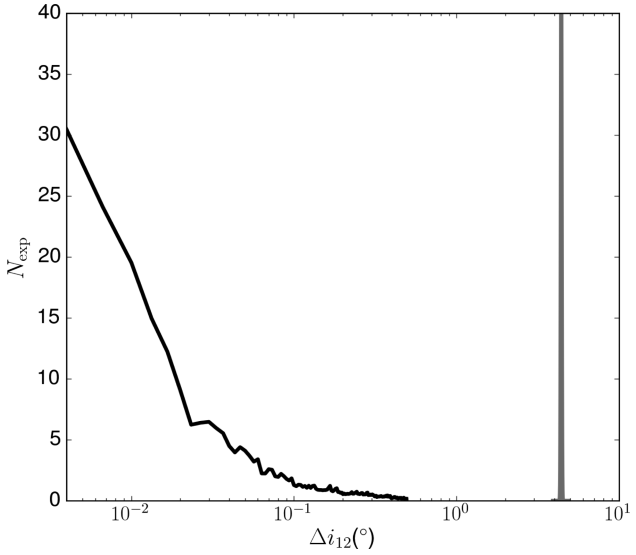

Figure 13. Predicted distribution of mutual inclinations between the two planets in the observed *Kepler* double transit population for different model populations that both produce the correct number of double and single transiting systems. The grey line refers to the model where the two planets are inherently inclined by $\Delta i_{12} = 4.^{\circ}4$. The black line refers to the model where the two planets are secularly perturbed by a outer companion with $m_3 = 1 M_{\rm J}$, $\Delta i = 10°$ and a_3=1.9 au.

inclination and a fraction $(1 - f)$ that are two-planet systems with an inclined outer companion. We can thus rewrite equation (26) as

$$N_{\rm sing,Kep} = N_{\rm sing,inh} + f(N_{\rm sing,Ndoub=341})_{\Delta i_{12}} + (1 - f)(N_{\rm sing,Ndoub=341})_{\rm planet}, \quad (27)$$

where $(N_{\rm sing,\ Ndoub\ =\ 341})_{\Delta i_{12}}$ is the number of singles that would have been produced from the population of two-planet systems with a fixed mutual inclination of Δi_{12}, had it been numerous enough to reproduce the 341 double transiting *Kepler* systems (which is shown in Fig. 10 as a function of Δi_{12}). Conversely, $(N_{\rm sing,\ Ndoub\ =\ 341})_{\rm planet}$ is the number of singles that would have been produced from the population of two-planet systems that are perturbed by an outer companion, had it been numerous enough to reproduce the 341 double transiting systems. We estimate the number of inherently single planet systems to be $N_{\rm sing,\ inh} = 447$ from Section 6.3. We note that $N_{\rm sing,\ inh}$ will change for different values of Δi_{12}; however, for simplicity, we keep it constant at 447.

For the assumed $N_{\rm sing,\ inh}$ and an assumed fixed mutual inclination for the fraction of the double transiting systems that are inherently inclined (f), equation (27) means that the number of single transiting systems observed by *Kepler* can be reproduced by a specific combination with the fraction of double transiting systems that have an outer planet $(1 - f)$ and the properties of these planetary systems that determine the ratio of single to double transiting systems from this population [i.e. $(N_{\rm sing,\ Ndoub\ =\ 341})_{\rm planet}$]. This combination is plotted in Fig. 12, which can be read alongside Fig. C1 to determine the outer planet parameters required to reproduce the required $(N_{\rm sing,\ Ndoub\ =\ 341})_{\rm planet}$. For example, for $f = 0.2$ and $\Delta i_{12} = 2°$, $(N_{\rm sing,\ Ndoub\ =\ 341})_{\rm planet} = 1676$ from Fig. 12, which from Fig. C1 would be reproduced by an outer planet with $a_3 = 2$ au, $m_3 = 132\ {\rm M}_{\oplus}$ and $\Delta i = 10°$. For $f = 0.5$, $(N_{\rm sing,\ Ndoub\ =\ 341})_{\rm planet}$ is increased to 2192, requiring the mass of this outer planet to be increased to $m_3 = 955\ {\rm M}_{\oplus}$ (for $a_3 = 2$ au and $\Delta i = 10°$). The outer planet parameters required to produce $(N_{\rm sing,\ Ndoub\ =\ 341})_{\rm planet}$ are therefore extremely sensitive to the value of f. However, increasing the value of Δi_{12} for a given value of f increases the value of $(N_{\rm sing,\ Ndoub\ =\ 341})_{\Delta i_{12}}$ and hence decreases $(N_{\rm sing,\ Ndoub\ =\ 341})_{\rm planet}$, as shown in Fig. 12, requiring an outer planet that is a weaker perturber of the inner planets.

It should be noted that f and $1 - f$ are not equivalent to the underlying fraction of stars that host a two-planet system with a fixed mutual inclination or a two-planet system with an outer companion, respectively. However, if f is known, such fractions for the underlying population of stars can be estimated through occurrence rate calculations. We discuss such calculations of occurrence rates in Section 7.3; however, it is first necessary to estimate a value for f, which we discuss below.

7.2 Comparing inherently mutually inclined and outer planet populations

From Section 6.3 a sole population of two-planet systems that are inherently mutually inclined by $\Delta i = 3.^{\circ}6$ (i.e. when $f = 1$) can reproduce a population of single and double transiting systems representative of those observed by *Kepler* (Fig. 9). However from Section 6.4 a sole population of two-planet systems with an outer planet (i.e. $f = 0$) can also reproduce a population of single and double transiting systems representative of those observed by *Kepler* (Fig. 11). Here we look to differentiate between these two models by considering the predicted distribution of mutual inclinations that would be observed in the two-planet populations for each model. We note that combining these two models in a way described in Section 7.1 (i.e. when $0 < f < 1$) would then give some intermediate distribution of mutual inclinations between the overall two-planet population.

For the model in which the two planets have an inherent mutual inclination of $\Delta i = 3.^{\circ}6$, that distribution is narrowly peaked at $3.^{\circ}6$ (see Fig. 13). In contrast, for the model in which two planets are perturbed by an inclined outer planet, the distribution of mutual inclinations is biased towards coplanar systems. This is because, while the outer planet induces a significant mutual inclination

between the inner planets, as required to reproduce the correct ratio of single to double transiting systems, the inclination is not always large (see Fig. 5), and the probability of witnessing a double transit system is much higher when their mutual inclination is low. Consider an outer companion with $m_3 = 24$ M$_\oplus$, $a_3 = 1.07$ au and $\Delta i = 10^\circ$, which was in a minimum of the modified χ^2 space (white circle, Fig. 11, top panel). Weighting the secularly evolving mutual inclinations between the inner two planets in the 341 considered systems by the associated double transit probability gives the predicted distribution of mutual inclinations that are most likely to be observed. This distribution is shown by the black line in Fig. 13. It is clear that the most likely observed mutual inclination is when the inner two planets are coplanar. Moreover, the number of systems expected to be observed with mutual inclinations beyond $0\overset{\circ}{.}5$ drops to negligible values.

From transit duration variation studies, the distribution of mutual inclinations between planets in multiplanet *Kepler* systems is peaked at $\sim 2^\circ$ (Fang & Margot 2012; Fabrycky et al. 2014), noting, however, that these works consider different planet populations from those considered here, as discussed in Section 6.3. Combining the two above-mentioned models to produce a similar distribution in mutual inclinations may therefore allow for f to be determined. We look to combine the two models in such a way to predict a value of f, as well as modelling the TDVs of the planetary systems considered in this work directly to predict the distribution of inherent mutual inclinations, as part of future work. For example, if a fraction of two-planet systems observed by *Kepler* are considered to have a fixed mutual inclination of $\Delta i_{12} = 4^\circ$, then in order to reproduce a distribution of mutual inclinations that peaks at $\sim 2^\circ$ from modelling of TDVs, it might be expected that $f \sim 0.5$.

An additional method to estimate f might be to consider whether hypothetical outer planets considered in this work would have been detectable by other means. It is expected that RV studies would be most sensitive to such outer planetary companions. In Fig. 11, we plot a rough constraint from RV studies, shown by the red dashed lines, assuming a detection threshold of ~ 2 m s^{-1}. Outside of 5 au we assume that RV studies are not sensitive to planets due to long periods. Planets above or to the left-hand side of these lines would therefore be detectable with this level of RV precision. This detection threshold suggests that a wide-orbit planet located in the minima of the modified χ^2 values in Fig. 11 (white circle) should be just detectable by RV studies. This would assume, however, that all *Kepler* systems with two planets host this outer companion, i.e. $f = 0$. From Fig. 12 and as highlighted in Section 7.1, if $f > 0$, then a planet with a larger mass, shorter period or larger inclination is required to reproduce the total number of single transiting systems observed by *Kepler*. Such outer planets should be readily detectable by RV surveys. For example, for the values of $f = 0.2$ and 0.5 for $\Delta i_{12} = 2^\circ$ considered in Section 7.1, both of the outer planets in these cases would be expected to be detectable by RV surveys. Due to the inherent faintness of *Kepler* stars, few have been extensively studied for wide-orbit planets. We suggest therefore that detailed follow-up RV studies of *Kepler* systems would allow for f to be constrained. Generally, for example, a low yield of outer planets in RV studies would suggest that f is low and vice versa.

7.3 Occurrence rates

Similar to that discussed specifically for *Kepler* systems in Section 7.1, consider that the underlying population of planetary systems contains three possible types of planetary systems. These include inherently single-planet systems, two-planet systems that have a fixed mutual inclination of Δi_{12} and two-planet systems that are being perturbed by an inclined outer planet. In Section 7.1, it was shown that combining these systems with a free parameter f, which describes the fraction of the observed double transiting population that are two-planet systems with a fixed mutual inclination, recovers the total number of single and double transiting systems observed by *Kepler*.

However, this value of f is not the same as the fraction of the underlying population of stars that have two planets that are inherently mutually inclined. Here we define the occurrence rate of a given population to be the fraction of stars that would be expected to host such systems. Occurrence rates in this work can be estimated by taking the ratio of the number of systems in a given model population ($N_{\rm mod}$) to the total number of stars observed by *Kepler* ($N_{\rm Kep}$). The individual occurrence rate for the inherently single planet systems is therefore given by $(N_{\rm mod}/N_{\rm Kep})_{\rm inh}$, for the two-planet systems with the fixed mutual inclination of Δi_{12} by $(N_{\rm mod}/N_{\rm Kep})_{\Delta i_{12}}$ and for the two-planet systems being perturbed by an inclined outer planet by $(N_{\rm mod}/N_{\rm Kep})_{\rm planet}$. For example, for the population of two-planet systems that were inherently mutually inclined by $3\overset{\circ}{.}6$ (for when $f = 1$), i.e. those which predicted a population of single transiting planets representative of those observed by *Kepler* (Section 6.3), the number of systems in the model population was equal to 43 807. From Section 6.1, the total number of *Kepler* stars was 164 966. Therefore, the occurrence rate for this type of system $(N_{\rm mod}/N_{\rm Kep})_{\Delta i_{12}} = 27$ per cent. Conversely, considering the population of two-planet systems that were perturbed by an outer companion with $m_3 = 24$ M$_\oplus$, $a_3 = 1.07$ au and $\Delta i = 10^\circ$ (white circle, Fig. 11, top panel) for when $f = 0$ predicted 42 733 systems in the associated model population. Therefore, the associated occurrence rate of this type of system $(N_{\rm mod}/N_{\rm Kep})_{\rm planet} = 26$ per cent.

The calculation of the occurrence rate for the population of inherently single planet systems is slightly different from that described above. From Section 6.3, assume that there are 447 inherently single planet systems (noting that this is subject to the value of Δi_{12}). The distribution of the semi-major axes of these 447 planets is equal to the difference between the distributions of semi-major axes for the single transiting systems observed by *Kepler* and those predicted by the population of two-planet systems with a fixed mutual inclination of $\Delta i_{12} = 3\overset{\circ}{.}6$, i.e. the difference between the left-hand panel of Fig. 8 and the bottom left-hand panel of Fig. 9. The number of inherently single planet systems in a model population is then the sum of the inverse of the single transit probabilities (R_*/a) of all these 447 planets. We find that this model population contains 15 852 systems, predicting an occurrence rate of inherently single planet systems of 9.6 per cent. This is large compared with the occurrence rate of hot Jupiters ($\sim$1–2 per cent, e.g. Marcy et al. 2005; Cumming et al. 2008; Mayor et al. 2011; Wright et al. 2012; Santerne et al. 2016). We therefore expect that our population of inherently single planet systems is dominated by a different population, such as those described in Section 6.1, which are poorly constrained.

In a similar way to that described for equation (27), the total occurrence rate of assumed planetary systems in the underlying population of planetary systems can be estimated to be

$$\left(\frac{N_{\rm mod}}{N_{\rm Kep}}\right)_{\rm tot} = \left(\frac{N_{\rm mod}}{N_{\rm Kep}}\right)_{\rm inh} + f\left(\frac{N_{\rm mod}}{N_{\rm Kep}}\right)_{\Delta i_{12}} + (1-f)\left(\frac{N_{\rm mod}}{N_{\rm Kep}}\right)_{\rm planet}. \quad (28)$$

Consider the example combination of systems from Section 7.2 for when $f = 0.2$, $\Delta i_{12} = 2^\circ$ and the outer planet parameters being $a_3 = 2$ au, $m_3 = 132\,\mathrm{M}_\oplus$ and $\Delta i = 10^\circ$. Here $f(N_{\rm mod}/N_{\rm Kep})_{\Delta i_{12}} \sim 3$ per cent and $(1 - f)(N_{\rm mod}/N_{\rm Kep})_{\rm planet} \sim 21$ per cent. We note that $f(N_{\rm mod}/N_{\rm Kep})_{\Delta i_{12}}/(1-f)(N_{\rm mod}/N_{\rm Kep})_{\rm planet} = 3/21 = 14$ per cent. This highlights that the occurrence rate of stars that have two-planet systems with an inherent mutual inclination is similar to but not the same as the parameter f.

Combining with the occurrence rate of inherently single planet systems estimated above, the total occurrence rate of planetary systems becomes 34 per cent. This is similar to occurrence rates of ∼25–30 per cent for *Kepler*-like planets derived from injection and recovery analysis of planet candidates from the Kepler pipeline (Petigura, Howard & Marcy 2013; Christiansen et al. 2015).

Estimates of occurrence rates for planets similar to the outer planets considered in this work exist from RV studies. Cumming et al. (2008) suggest an occurrence rate of 7.0 ± 1.4 per cent for planets with masses and semi-major axes of $m_{\rm p} = 1$–$10 M_{\rm J}$ and ∼1–5 au, respectively. Extrapolating this occurrence rate also predicts that 17–20 per cent of stars have gas giants within 20 au. Similarly, Mayor et al. (2011) suggest an occurrence rate of 13.9 ± 1.7 per cent for planets with masses and periods of $m_{\rm p} > 50\,\mathrm{M}_\oplus$ and $P < 10$ yr, respectively. More recently, Bryan et al. (2016) suggest that for systems with one or two RV planets, the occurrence rate of an additional companion with a mass and semi-major axis of 1–$20 M_{\rm J}$ and 5–20 au, respectively, is as high as 52 ± 5 per cent. The above example occurrence rate for the systems with an outer planet, i.e. $(1 - f)(N_{\rm mod}/N_{\rm Kep})_{\rm planet} \sim 21$ per cent, is then therefore not contradicted by these studies. However, this example assumed an estimated value of f. In addition to the methods described in Section 7.2, observationally estimated occurrence rates for outer planets may also be able to constrain the value of f. For example, if it is assumed that the occurrence rate of the types of outer planets considered in this work is 13.9 per cent (Mayor et al. 2011), then it can be estimated that $(1 - f)(N_{\rm mod}/N_{\rm Kep})_{\rm planet} \sim 13.9$ per cent. As $(N_{\rm mod}/N_{\rm Kep})_{\rm planet} \not> 1$ (i.e. it is unphysical that there are more stars in the model population than the number actually observed by *Kepler*), this results in an upper limit of $f \leq 0.86$. We therefore suggest that combining this method of placing constraints on f with those described in Section 7.2 might provide a strong constraint on the percentage of planetary systems that may share a fixed mutual inclination compared with systems that may host an outer inclined planet.

7.4 Comparing with similar works

Whether an outer planet can reduce the multiplicity of expected transiting planets in an inner planetary system in the context of N-body simulations has recently been investigated by Hansen (2017). A notable example they include is the effect of a companion with a mass of $1 M_{\rm J}$ at 1 au, which is inclined to an inner population of planetary systems with a variety of multiplicities by 10°. They find that the ratio of the total number of double to single transiting systems that *Kepler* would be expected to observe is 0.184 (i.e. approximately five times more expected single than double transiting systems). We find that an identical outer planetary companion in our work gives this ratio to be 0.14. We suggest this difference is caused by the population of inner planetary systems used. Hansen (2017) incorporate 50 model inner planetary systems with a range of multiplicities (the vast majority contained three to six planets at the end of their simulations), rather than the two-planet *Kepler* systems considered in this work. Higher multiplicities increase the number of competing secular modes in the system, which can stabilize inner planets against the secular perturbations of an outer companion (e.g. Read & Wyatt 2016). Such an example was shown in this work in Section 5 for application to Kepler-48. Perhaps then, mutual inclinations are more easily induced between inner planets in this work, increasing the predicted number of single transiting planets that *Kepler* would be expected to observe, relative to a fixed population of planetary systems.

Moreover, compared with N-body simulations, our work does not allow for dynamical instability. If inclinations are large, then they couple with eccentricity (Murray & Dermott 1999), potentially causing orbital crossings between neighbouring planets, leading to dynamical instabilities on short, non-secular time-scales. Indeed, Hansen (2017) find for the above-mentioned outer planetary companion that roughly half of the 50 systems they consider lose at least one planet. Moreover, Pu & Wu (2015) suggest that the abundance of single and double transiting systems might be the remains of higher order planetary systems that were once tightly packed and have since undergone dynamical instability. A detailed discussion on how dynamical stability would be expected to affect our results is difficult. Our choice that all planets must be initially Hill stable is by no means a robust constraint on the long-term stability of all the planetary systems we consider during the secular interaction.

The effects of dynamical instability in tightly packed planet systems interacting with a wide-orbit companion planet were also shown by Mustill et al. (2015). They find that an outer giant planet undergoing Kozai–Lidov interactions with a stellar binary (Kozai 1962; Lidov 1962) can have an eccentricity that takes its orbit within the inner planets, leading to a significant reduction in planet multiplicity. Moreover, more recent work in Mustill et al. (2016) suggests that these same interactions can cause ∼50 per cent of *Kepler*-like systems to lose a planet, either through collisions or ejections. If inclination is not completely decoupled with eccentricity, then these works suggest that dynamical instability plays a significant role in sculpting an inner planetary system.

7.5 Metallicity distribution

The fraction of stars with gas giants increases with higher metal content (e.g. Gonzalez 1997; Thorngren et al. 2016). However, it is unclear if this relation extends to smaller planets with $R_{\rm p} \lesssim 4\,\mathrm{R}_\oplus$ (Mayor et al. 2011; Zhu, Wang & Huang 2016). If single transiting planets are in systems that contain an outer giant companion similar to that considered in this work, then the transiting planet should follow a similar metallicity relation to the giant planet. If there is an inherent population of single-planet systems with $R_{\rm p} \lesssim 4\,\mathrm{R}_\oplus$, in addition to a population of inherently mutually inclined double transiting systems, then these systems will follow a different metallicity relation. Therefore, the population of single and double transiting systems observed by *Kepler* may contain a mixture of metallicity relations. If a distinction can be made between these different relations, then this may place constraints on the presence of additional planets in *Kepler* systems with a single transiting planet.

7.6 Assumptions of this work

Throughout this work, we have considered that mutual inclinations evolve between two planets due to secular interactions with an outer planet. As stated above, increasing the multiplicity of planetary systems complicates the evolution of mutual inclinations. For application to the Kepler Dichotomy, including higher multiplicity systems may cause proportionally fewer to be observed as single

transiting systems. We look to investigate this as part of future work. Moreover, higher multiplicity systems also allow for investigation into whether the presence of an outer planetary companion can explain the number of higher order systems observed by *Kepler*. This is of particular interest as Johansen et al. (2012) find that generating a model population that predicts the number of systems observed by *Kepler* with three transiting planets (with small inherent mutual inclinations and no outer companion) cannot simultaneously predict the number of systems with a single and two transiting planets observed by *Kepler*.

We have also assumed that the inner transiting planets interacting with an outer companion were initially coplanar. However, these transiting planets would most likely also have a small inherent mutual inclination (e.g. Fang & Margot 2012; Fabrycky et al. 2014), which, in turn, may affect the mean double transit probability.

8 SUMMARY AND CONCLUSIONS

In summary, during the first part of this work, we developed a semi-analytical method for the calculation of transit probabilities by considering the area a transiting planet subtends on a celestial sphere (Section 2). Applying this method to a general two-planet system, we showed how the probability that both planets are observed to transit changes as they become mutually inclined.

In Section 3, we discussed how the mutual inclination between two initially coplanar planets evolves due to secular interactions with an external mutually inclined planetary companion. We derived the full solution describing this evolution assuming that the mutual inclination remains small, before simplifying it under the assumption that the external planet was on a wide orbit. We found that the maximum mutual inclination between the inner two planets is approximately equal to twice the initial mutual inclination with the external planet. Below this, the maximum mutual inclination between the inner two planets scales according to the mass, semi-major axis and inclination of the external planet by $\propto \Delta i m_3/a_3^3$.

How the secular interaction causes the double transit probability of the inner two planets to evolve was shown in Section 4. Assuming that this double transit probability is significantly reduced when the maximum mutual inclination exceeds $\approx(R_*/a_1) + (R_*/a_2)$, we derived an expression for the mean of the double transit probability considering a given external planetary companion. This expression was applied to Kepler-56, Kepler-68 and Kepler-48 to place constraints on the inclination of the outer RV-detected planets in these systems in Section 5. We found that the inner two transiting planets in Kepler-56 and Kepler-68 are not significantly secularly perturbed by the outer planets, regardless of their inclination. For HD 106315, we found that an outer planet inferred from recent RV analysis can cause a significant perturbation to the mutual inclination of two internal transiting planets. Moreover, we found that if the outer planet is present within $\sim$1 au, its inclination must be no more than $2\overset{\circ}{.}4$; otherwise, the probability of observing both the inner planets to transit is significantly reduced. We also found that the RV-detected planet in Kepler-48 needs to be inclined with respect to the inner planets by $\lesssim 3\overset{\circ}{.}7$; otherwise, the probability that all the inner planets are observed to transit is significantly reduced. We conclude therefore that using the expression for the mean transit probability between inner planets from equation (20) and (17) can be used to place significant constraints on the inclinations of RV-detected planets, whose host systems also contain transiting planets.

We further applied our method of calculating transit probabilities to the *Kepler* population in Section 6. We found that relative to a fixed population of transiting systems with two planets on initially coplanar orbits, the expected number of single transiting systems can be significantly increased both by inherently inclining the two planets and by introducing an outer planetary companion. We found that an inherent mutual inclination of $\Delta i_{12} = 3\overset{\circ}{.}6$ predicts a population of single transiting planets most representative of those in the *Kepler* population. Moreover, we found that outer planets initially inclined by $\sim 3^\circ$–10° to the inner planets also predict a representative population of single transiting systems. These outer planets should be detectable by RV studies.

However, it is likely that planetary systems observed by *Kepler* may include a combination of systems that include inherently single planet systems, two-planet systems that have some fixed mutual inclination and two-planet systems interacting with an inclined outer planet. For two-planet systems that are perturbed by an outer planet, the distribution of the mutual inclinations between the inner planets of such systems is biased towards coplanar systems. This is due to an increased probability of observing inner planets when coplanar compared with when mutual inclinations are larger. We suggest that combining populations of inherently mutually inclined two-planet systems with two-planet systems that are interacting with an outer planet may be able to reproduce the observed distribution of mutual inclinations between *Kepler* planets. In doing so, this may provide constraints on the presence of outer planets in the *Kepler* population. We suggest also that a detailed follow-up of RV studies in *Kepler* systems will provide more direct constraints on the presence of outer planets. There should also be a dichotomy in the number of transiting systems observed by the upcoming *TESS* mission (Ricker et al. 2014); however, for these systems, astrometry and RV techniques will be able to be used to verify the presence and influence of outer planets.

ACKNOWLEDGEMENTS

We thank Simon Gibbons and Grant Kennedy for useful conversations regarding this work. MJR acknowledges support of an STFC studentship, and MCW acknowledges the support from the European Union through grant number 279973. We also thank the reviewer for comments, which were a great help in improving this paper. This research has also made use of the NASA Exoplanet Archive, which is operated by the California Institute of Technology, under contract with the National Aeronautics and Space Administration under the Exoplanet Exploration Program.

REFERENCES

Almenara J. M., Díaz R. F., Bonfils X., Udry S., 2016, A&A, 595, L5
Ballard S., Johnson J. A., 2016, ApJ, 816, 66
Becker J. C., Adams F. C., 2016, MNRAS, 455, 2980
Becker J. C., Vanderburg A., Adams F. C., Rappaport S. A., Schwengeler H. M., 2015, ApJ, 812, L18
Borucki W. J., Summers A. L., 1984, Icarus, 58, 121
Borucki W. J. et al., 2011, ApJ, 728, 117
Brakensiek J., Ragozzine D., 2016, ApJ, 821, 47
Bryan M. L. et al., 2016, ApJ, 821, 89
Casertano S. et al., 2008, A&A, 482, 699
Chambers J. E., 1999, MNRAS, 304, 793
Chen J., Kipping D., 2017, ApJ, 834, 17
Christiansen J. L. et al., 2015, ApJ, 810, 95
Ciceri S., Lillo-Box J., Southworth J., Mancini L., Henning T., Barrado D., 2015, A&A, 573, L5
Coughlin J. L. et al., 2014, AJ, 147, 119
Coughlin J. L. et al., 2016, ApJS, 224, 12
Crossfield I. J. M. et al., 2017, preprint (arXiv:1701.03811)

Cumming A., Butler R. P., Marcy G. W., Vogt S. S., Wright J. T., Fischer D. A., 2008, PASP, 120, 531
Dawson R. I., Chiang E., 2014, Science, 346, 212
de Bruijne J. H. J., 2012, Ap&SS, 341, 31
Désert J.-M. et al., 2015, ApJ, 804, 59
Dressing C. D., Charbonneau D., 2015, ApJ, 807, 45
Fabrycky D. C. et al., 2014, ApJ, 790, 146
Fang J., Margot J.-L., 2012, ApJ, 761, 92
Figueira P. et al., 2012, A&A, 541, A139
Fragner M. M., Nelson R. P., 2010, A&A, 511, A77
Fressin F. et al., 2013, ApJ, 766, 81
Gaia Collaboration et al., 2016, A&A, 595, A2
Gilliland R. L. et al., 2013, ApJ, 766, 40
Gonzalez G., 1997, MNRAS, 285, 403
Hadden S., Lithwick Y., 2014, ApJ, 787, 80
Hansen B. M. S., 2017, MNRAS, 467, 1531
Holczer T. et al., 2016, ApJS, 225, 9
Huang C. X., Petrovich C., Deibert E., 2016, preprint (arXiv:1609.08110)
Huber D. et al., 2013, ApJ, 767, 127
Johansen A., Davies M. B., Church R. P., Holmelin V., 2012, ApJ, 758, 39
Kane S. R., 2015, ApJ, 814, L9
Kozai Y., 1962, AJ, 67, 579
Lai D., Pu B., 2017, AJ, 153, 42
Li G., Naoz S., Valsecchi F., Johnson J. A., Rasio F. A., 2014, ApJ, 794, 131
Lidov M. L., 1962, Planet. Space Sci., 9, 719
Lillo-Box J. et al., 2014, A&A, 562, A109
Lissauer J. J. et al., 2011, ApJS, 197, 8
Lissauer J. J. et al., 2014, ApJ, 784, 44
Lopez E. D., Rice K., 2016, preprint (arXiv:1610.09390)
Malmberg D., Davies M. B., Heggie D. C., 2011, MNRAS, 411, 859
Marcy G., Butler R. P., Fischer D., Vogt S., Wright J. T., Tinney C. G., Jones H. R. A., 2005, Prog. Theor. Phys. Suppl., 158, 24
Marcy G. W. et al., 2014, ApJS, 210, 20
Marmier M. et al., 2013, A&A, 551, A90
Mayor M. et al., 2011, preprint (arXiv:1109.2497)
Morton T. D., 2012, ApJ, 761, 6
Morton T. D., Johnson J. A., 2011, ApJ, 738, 170
Morton T. D., Bryson S. T., Coughlin J. L., Rowe J. F., Ravichandran G., Petigura E. A., Haas M. R., Batalha N. M., 2016, ApJ, 822, 86
Murray C. D., Dermott S. F., 1999, Solar System Dynamics. Cambridge Univ. Press, Cambridge
Mustill A. J., Davies M. B., Johansen A., 2015, ApJ, 808, 14
Mustill A. J., Davies M. B., Johansen A., 2016, preprint (arXiv:1609.08058)
Otor O. J. et al., 2016, AJ, 152, 165
Pepper J. et al., 2016, preprint (arXiv:1607.01755)
Perryman M. A. C. et al., 2001, A&A, 369, 339
Perryman M., Hartman J., Bakos G. Á., Lindegren L., 2014, ApJ, 797, 14
Petigura E. A., 2015, PhD thesis, Univ. California
Petigura E. A., Howard A. W., Marcy G. W., 2013, Proc. Natl. Acad. Sci., 110, 19273
Pu B., Wu Y., 2015, ApJ, 807, 44
Quinn S. N. et al., 2015, ApJ, 803, 49
Ragozzine D., Holman M. J., 2010, preprint (arXiv:1006.3727)
Read M. J., Wyatt M. C., 2016, MNRAS, 457, 465
Ricker G. R. et al., 2014, Proc. SPIE, 9143E, 914320
Rodriguez J. E. et al., 2017, preprint (arXiv:1701.03807)
Rogers L. A., 2015, ApJ, 801, 41
Rowan D. et al., 2016, ApJ, 817, 104
Rowe J. F. et al., 2015, ApJS, 217, 16
Rowe J. F. et al., 2014, ApJ, 784, 45
Sahlmann J., Triaud A. H. M. J., Martin D. V., 2015, MNRAS, 447, 287
Santerne A. et al., 2016, A&A, 587, A64
Schneider J., Dedieu C., Le Sidaner P., Savalle R., Zolotukhin I., 2011, A&A, 532, A79
Seader S. et al., 2015, ApJS, 217, 18
Sozzetti A., Giacobbe P., Lattanzi M. G., Micela G., Morbidelli R., Tinetti G., 2014, MNRAS, 437, 497
Steffen J. H., Coughlin J. L., 2016, Proc. Natl. Acad. Sci., 113, 12023
Steffen J. H. et al., 2012, Proc. Natl. Acad. Sci., 109, 7982
Steffen J. H. et al., 2013, MNRAS, 428, 1077
Thorngren D. P., Fortney J. J., Murray-Clay R. A., Lopez E. D., 2016, ApJ, 831, 64
Tremaine S., Dong S., 2012, AJ, 143, 94
Van Eylen V., Albrecht S., 2015, ApJ, 808, 126
Weiss L. M., Marcy G. W., 2014, ApJ, 783, L6
Weiss L. M. et al., 2016, ApJ, 819, 83
Winn J. N. et al., 2009, ApJ, 700, 302
Wittenmyer R. A. et al., 2016, ApJ, 819, 28
Wolfgang A., Rogers L. A., Ford E. B., 2016, ApJ, 825, 19
Wright J. T., Upadhyay S., Marcy G. W., Fischer D. A., Ford E. B., Johnson J. A., 2009, ApJ, 693, 1084
Wright J. T., Marcy G. W., Howard A. W., Johnson J. A., Morton T. D., Fischer D. A., 2012, ApJ, 753, 160
Youdin A. N., 2011, ApJ, 742, 38
Zakamska N. L., Tremaine S., 2004, AJ, 128, 869
Zhu W., Wang J., Huang C., 2016, ApJ, 832, 196

APPENDIX A: FURTHER DISCUSSION OF TRANSIT EQUATIONS

A1 Central transit line

The centre of the transit region is defined by equation (2) as

$$-\sin\Delta i\sin\theta\sin\phi+\cos\Delta i\cos\theta=0.$$

Assuming that $\phi=0\rightarrow2\pi$ and that a corresponding value of θ for each value of ϕ can be in the range of $0<\theta<\pi$, equation (2) can be rearranged to give

$$\theta=\arctan\left(\frac{1}{\tan\Delta i\sin\phi}\right)\quad\text{for }\phi<\pi,$$
$$\theta=\pi+\arctan\left(\frac{1}{\tan\Delta i\sin\phi}\right)\quad\text{for }\phi>\pi. \tag{A1}$$

A2 Upper transit boundary

The upper boundary of a transit region is given by equation (4) as

$$-\sin\Delta i\sin\theta_2\sin\phi_2+\cos\Delta i\cos\theta_2=-\chi.$$

A value of θ_2 for a given ϕ_2 can be calculated through solving a quadratic of the form

$$\left(A^2+B^2\right)x^2+2A\chi x+\chi^2-B^2=0, \tag{A2}$$

where

$$x=\sin\theta_2,\quad A=-\sin\Delta i\sin\phi_2,\quad B=\cos\Delta i.$$

Depending on the value of Δi, the calculation of θ_2 for a given value of ϕ_2 can be grouped into three different regimes: (1) Δi is small enough that the upper boundary of the transit region never crosses the fixed reference plane. (2) Δi is large enough that the upper boundary of the transit region does cross the fixed reference plane. (3) For high values of Δi, the upper transit boundary has values of θ_2 only for $0<\phi_2<\pi$. This can be thought of as the transit region going over the pole of the celestial sphere.

For regime (1), the value of θ_2 for a given ϕ_2 is equivalent to that obtained from the positive root of equation (A2), mirrored about $\pi/2$. The transition to regime (2) occurs for when the upper transit boundary first crosses the fixed reference plane. Here

$\Delta i = \arcsin(\chi)$. As Δi is increased beyond this value, the intersection between the upper transit boundary and the fixed reference plane occurs at $\phi_2 = \phi_0$ and $\phi_2 = \pi - \phi_0$, for which $\theta_2 = \pi/2$. From equation (4) ϕ_0 is given by $\phi_0 = \arcsin(\chi / \sin \Delta i)$. Therefore, $\theta_2 < \pi/2$ for $\phi_0 < \phi_2 < \pi - \phi_0$ and $\theta_2 > \pi/2$ otherwise. When $\phi_0 < \phi_2 < \pi - \phi_0$, θ_2 is hence obtained from the positive solution of equation (A2) and by the positive solution mirrored about $\pi/2$ otherwise.

Finally, the transition to regime (3) occurs when $\Delta i = \arccos(\chi)$. Similarly to regime (2), as Δi is increased beyond this value, the upper transit boundary crosses the fixed reference plane at $\phi_2 = \phi_0$ and $\phi_2 = \pi - \phi_0$, and hence θ_2 is defined only for when $\phi_0 < \phi_2 < \pi - \phi_0$. The solution from equation (A2), which gives the smaller value θ_2, corresponds to $\theta_2 > \pi/2$ values and needs to be mirrored about $\pi/2$, with the solution giving the larger value of θ_2 corresponding to $\theta_2 < \pi/2$ values.

To summarize, consider that for a given value of ϕ_2, equation (A2) gives two solutions for θ_2, denoted as θ_2^{*1} and θ_2^{*2}, respectively. For $\Delta i < \arcsin(\chi)$,

$$\theta_2 = \frac{\pi}{2} + \left(\frac{\pi}{2} - \theta_2^{*1}\right) \quad \text{for } 0 < \phi_2 < 2\pi, \tag{A3}$$

where $\theta_2^{*1} > 0$ and $\theta_2^{*2} < 0$.

For $\arcsin(\chi) < \Delta i < \arccos(\chi)$,

$$\theta_2 = \theta_2^{*1} \quad \text{for } \phi_0 < \phi_2 < \pi - \phi_0,$$

$$\theta_2 = \frac{\pi}{2} + \left(\frac{\pi}{2} - \theta_2^{*1}\right) \quad \text{otherwise,} \tag{A4}$$

where $\theta_2^{*1} > 0$, $\theta_2^{*2} < 0$ and $\phi_0 = \arcsin(\chi / \sin \Delta i)$.

For $\Delta i > \arccos(\chi)$,

$$\theta_2 = \max\left(\theta_2^{*1}, \theta_2^{*2}\right)$$

$$\text{and} \quad \text{for } \phi_0 < \phi_2 < \pi - \phi_0$$

$$\theta_2 = \frac{\pi}{2} + \left(\frac{\pi}{2} - \min\left(\theta_2^{*1}, \theta_2^{*2}\right)\right), \tag{A5}$$

where $\theta_2^{*1} > 0$, $\theta_2^{*2} > 0$.

A3 Lower transit boundary

The lower boundary of the transit region is given by equation (3) as

$$-\sin \Delta i \sin \theta_1 \sin \phi_1 + \cos \Delta i \cos \theta_1 = \chi.$$

Depending on the value of Δi, the calculation θ_1 for a given ϕ_1 can be grouped into the same regimes as described for the upper transit boundary. However, now in regime (1), $\theta_1 < \pi/2$ for $0 < \phi_1 < 2\pi$, in regime (2), the lower transit boundary crosses the fixed reference plane at $\phi_1 = \pi + \phi_0$ and $\phi_1 = 2\pi - \phi_0$, and in regime (3), θ_1 is defined only for $\pi + \phi_0 < \phi_1 < 2\pi - \phi_0$. Assuming that θ_1^{*1} and θ_1^{*2} are the solutions for θ_1 for a given ϕ_1 in the modified form of equation (A2), then following the same discussion as for the upper transit boundary it can be shown that for $\Delta i < \arcsin(\chi)$,

$$\theta_1 = \theta_1^{*1} \quad \text{for } 0 < \phi_1 < 2\pi, \tag{A6}$$

where $\theta_1^{*1} > 0$ and $\theta_1^{*2} < 0$.

For $\arcsin(\chi) < \Delta i < \arccos(\chi)$,

$$\theta_1 = \frac{\pi}{2} + \left(\frac{\pi}{2} - \theta_1^{*1}\right) \quad \text{for } \phi_0 + \pi < \phi_1 < 2\pi - \phi_0,$$

$$\theta_1 = \theta_1^{*1} \quad \text{otherwise,} \tag{A7}$$

where $\theta_1^{*1} > 0$, $\theta_1^{*2} < 0$ and $\phi_0 = \arcsin(\chi / \sin \Delta i)$.

For $\Delta i > \arccos(\chi)$,

$$\theta_1 = \min\left(\theta_1^{*1}, \theta_1^{*2}\right)$$

$$\text{and} \quad \text{for } \phi_0 + \pi < \phi_1 < 2\pi - \phi_0$$

$$\theta_1 = \frac{\pi}{2} + \left(\frac{\pi}{2} - \max\left(\theta_1^{*1}, \theta_1^{*2}\right)\right), \tag{A8}$$

where $\theta_1^{*1} > 0$, $\theta_1^{*2} > 0$.

APPENDIX B: SECULAR SOLUTION FOR MUTUAL INCLINATION EVOLUTION

From equation (11), the evolution of complex inclinations according to Laplace–Lagrange theory is given by

$$y_j(t) = \sum_{k=1}^{N} I_{jk} e^{i(f_k t + \gamma_k)}, \tag{B1}$$

where I_{jk} are the eigenvectors of the matrix $\mathbf{B}$ from equation (9) scaled to initial boundary conditions, f_i are the eigenfrequencies of $\mathbf{B}$ and γ_k are initial phase terms. If it is assumed that all the planets and the star are point masses and that the invariable plane is taken as a reference plane, it follows that $f_3 = 0$ and $I_{j3} = 0$. From the initial conditions, $|y_1(0)| = |y_2(0)| = i_1$. Hence, the complex inclinations of the inner two planets, respectively, are given by

$$y_1(t) = I_{11} \exp(i(f_1 t + \pi)) + I_{12} \exp(i(f_2 t)), \tag{B2}$$

$$y_2(t) = I_{21} \exp(i(f_1 t + \pi)) + I_{22} \exp(i(f_2 t)). \tag{B3}$$

Also from the initial conditions $-I_{11} + I_{12} = i_1$ and $-I_{21} + I_{22} = i_1$. The complex mutual inclination between the inner two planets is equivalent to

$$y_1(t) - y_2(t) = (I_{12} - I_{22}) \left[\exp(i(f_1 t + \pi)) + \exp(i f_2 t)\right]. \tag{B4}$$

Solving equation (11), we propose a set of variables to represent the full solution of I_{12} and I_{22},

$$K_{1m} = \frac{B_{13} B_{32}}{f_m + B_{31} + B_{32}},$$

$$K_{2m} = \frac{B_{13} B_{31}}{f_m + B_{31} + B_{32}},$$

$$K_{3m} = f_m + B_{12} + B_{13},$$

$$K_{4m} = f_m + B_{31} + B_{32}, \tag{B5}$$

where $m = 1, 2$,

$$R_{1(3-m)} = \frac{K_{3m} - K_{2m}}{B_{12} + K_{1m}},$$

$$R_{2(3-m)} = B_{31} + B_{32} R_{1(3-m)}, \tag{B6}$$

$$\epsilon = R_{11} + \frac{R_{21}}{K_{42}} (R_{12} - 1) + \frac{R_{22}}{K_{41}} (1 - R_{11}) - R_{12}. \tag{B7}$$

Hence, the components of the eigenvector associated with the f_2 eigenfrequency are given by

$$I_{12} = \frac{1}{\epsilon} [\Delta i (1 - R_{12})],$$

$$I_{22} = \frac{R_{11}}{\epsilon} [\Delta i (1 - R_{12})]. \tag{B8}$$

The non-zero f_1 and f_2 eigenfrequencies of the matrix $\mathbf{B}$ from equation (9) can be obtained by solving a quadratic of the

form

$$f^2 + f(B_{12} + B_{12} + B_{21} + B_{23} + B_{31} + B_{32}) + [B_{12}(B_{23} + B_{31} + B_{32}) + B_{13}(B_{21} + B_{23} + B_{32}) + B_{21}(B_{31} + B_{32}) + B_{23}B_{31}] = 0. \quad \text{(B9)}$$

We note that the solution given by equation (B8) recovers exactly what is predicted when solving equation (11) by numerical methods. The full solution that describes the mutual inclination between the inner two planets according to Laplace–Lagrange theory is therefore given by

$$y_1 - y_2 = \frac{\Delta i(1 - R_{12})(1 - R_{11})}{\epsilon}\left[e^{i(f_1 t + \pi)} + e^{i f_2 t}\right], \quad \text{(B10)}$$

with the variable K used in Section 3.2 being equivalent to $(1 - R_{12})(1 - R_{11})/\epsilon$.

APPENDIX C: REPRODUCING THE TOTAL NUMBER OF SINGLE TRANSITING PLANETS OBSERVED BY *KEPLER*

In Section 6, we considered *Kepler* systems with two transiting planets that are secularly interacting with an outer planet on an inclined orbit. We found that the number of single transiting systems *Kepler* would be expected to observe can be dramatically increased as a result of this interaction. Fig. C1 shows the total number of single transiting objects *Kepler* would be expected to observe from the method outlined in Section 6.4, for when the outer planet has the same parameters as the respective panels of Fig. 11. Again for $\Delta i \gg 20^\circ$, Laplace–Lagrange theory is expected to break down and is included for completeness. The white line gives where the total number of single transiting planets *Kepler* would be expected to observe from the model population is equal to the number in the *Kepler* population, i.e. 1951. The red dashed lines give an estimate for an RV detection threshold.

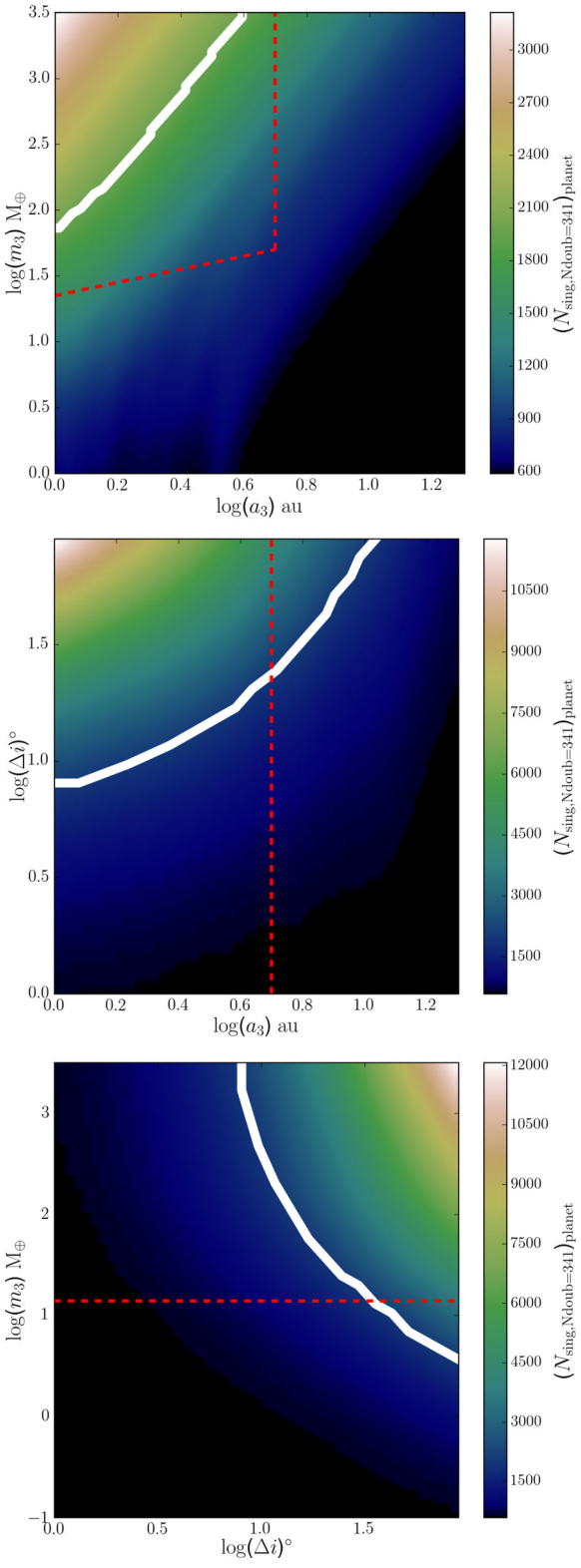

Figure C1. The total number of single transiting planets *Kepler* would be expected to observe for given third planet parameters. The white line corresponds to the total number of single transiting systems currently observed by *Kepler* (1951). The red lines give an estimate for the detection threshold of RV surveys.

This paper has been typeset from a TEX/LATEX file prepared by the author.